

Fantômas Unconfined: global QCD fits with Bézier parameterizations

Lucas Kotz^{a,1}, Aurore Courtoy^{b,2,*}, T. J. Hobbs^{c,3}, Pavel Nadolsky^{d,4,**}, Fredrick Olness^{a,5},
Maximiliano Ponce-Chavez^d, Varada Purohit^a

^aDepartment of Physics, Southern Methodist University, Dallas, 75275-0175, TX, USA

^bInstituto de Física, Universidad Nacional Autónoma de México, Apartado Postal 20-364, Ciudad de México, 01000, Mexico

^cHigh Energy Physics Division, Argonne National Laboratory, Lemont, 60439, IL, USA

^dDepartment of Physics and Astronomy, Michigan State University, East Lansing, 48824, MI, USA

Abstract

Fantômas is a C++ toolkit for exploring the parametrization dependence of parton distribution functions (PDFs) and other correlator functions in quantum chromodynamics (QCD). Fantômas facilitates the generation of adaptable polynomial parametrizations for PDFs, called metamorphs, to find best-fit PDF solutions and quantify the epistemic uncertainty associated with the parametrizations during their fitting. The method employs Bézier curves as universal approximators for a variety of PDF shapes. Integrated into the xFitter framework for the global QCD analysis, Fantômas provides a foundation for general models of PDFs, while reducing the computational time compared to the approaches utilizing traditional polynomial parametrizations as well as providing an interpretable alternative to neural-network-based models. This paper outlines the structure and practical usage of the Fantômas toolkit, including its inputs, outputs, and implementation within xFitter. It also provides a practical example of using Fantômas for uncertainty quantification as well as the combination of PDF fits into a single ensemble.

Keywords: hadron structure, parton distributions, Bézier curves, universal approximation

PROGRAM SUMMARY

Program Title: Fantômas

CPC Library link to program files: (to be added by Technical Editor)

Developer's repository link: <https://gitlab.com/cteq-tea/public/fantomas4qcd>
<https://gitlab.cern.ch/fitters/xfitter/> in the **Fantomas** branch.

Licensing provisions(please choose one): CC0 1.0/CC BY 4.0/MIT/Apache-2.0/BSD 3-clause/BSD 2-clause/GPLv3/GPLv2/LGPL/CC BY NC 3.0/MPL-2.0

Programming language: C++

Supplementary material:

Nature of problem: Dependence on functional forms of parton distribution functions (PDFs) in a hadron introduces a significant uncertainty in precision predictions for many high-energy scattering processes. A new generation of global analyses of PDFs requires streamlined, fast generation of diverse functional forms satisfying number and momentum sum rules consistent with QCD, asymptotic limits, integrability of PDFs, and positivity of the resulting cross sections. Other approaches to approximate a variety of PDFs may lack parsimony and interpretability attributed to explicit functional forms.

Solution method: The Fantômas toolkit provides a framework to construct families of increasingly flexible parametrizations for PDFs using Bézier curves. These polynomial functions are universal approximators that are computed from the values of the function itself at user-specified control points. Fantômas provides a method to cast many existing PDF parametrizations into an internal format (a metamorph) that simplifies raising the degree of the polynomial solely by adding new control points, without refitting all PDF parameters from scratch. The Fantômas approach systematizes exploration of the multidimensional parameter landscape of PDFs while potentially reducing human involvement and computing time compared to traditional realizations.

Additional comments including restrictions and unusual features (approx. 50-250 words):

Preprint numbers: ANL-197925


Contents


1	Introduction	3
2	Functional forms for PDFs	4
2.1	The role of parametrization studies in modern PDF fits	4
2.2	Metamorph	5
2.3	Sum rules and prior constraints	7
3	The Fantômas toolkit	7
3.1	Classes	8
3.2	The core source files, steering cards	9
3.2.1	Example of a steering card	10
3.3	The fitting algorithm	10
3.4	The C wrapper	12
3.5	The standalone Fantômas implementation	12
3.6	The xFitter implementation	14
3.6.1	Core files	14
3.6.2	χ^2 penalties	15
3.6.3	More on inputs and outputs	16
4	Practical example: pion PDFs	17
4.1	Building up a metamorph	17
4.2	Exploring the pion fits	20
4.3	Channeling flexibility	22
5	Combination of PDF fits	23
5.1	Procedure A. A PDF combination with aleatoric and epistemic uncertainties.	24
5.2	Procedure B. Including uncertainties from other nonperturbative functions	24
6	Guidelines	25
7	Conclusions	26
Appendix A	Review of the xFitter framework	27
Appendix B	Numerical artifacts	29
Appendix B.1	Parametric vs. 1D Bézier curves	30
Appendix B.2	Condition Number and Matrix Inversion in Polynomial Interpolation	30
Appendix B.3	Runge Phenomenon in Polynomial Interpolation	30
Appendix C	A Mathematica implementation	31


*aurore@fisica.unam.mx


**nadolsky@smu.edu


¹  0009-0007-5639-0350

²  0000-0002-1825-0097

³  0000-0002-2729-0015

⁴  0000-0003-3732-0860

⁵  0000-0001-6799-2436

⁶  0009-0003-0139-4072

1. Introduction

The phenomenology of hadron structure is a burgeoning subdiscipline of quantum chromodynamics (QCD) linking strong interactions in low- and high-energy domains. Determination of parton distribution functions (PDFs) in nucleons, mesons, and nuclei is advancing rapidly with the influx of experimental measurements, multiloop theoretical calculations, and lattice QCD computations of quantities which can be related to the PDFs [1–3]. While the dependence of a PDF $f_a(x, Q)$ on the factorization energy scale Q is precisely specified by perturbative QCD, its dependence on x — the momentum fraction that a parton a carries inside the parent hadron — is fully non-perturbative and is currently inferred either from experimental data using the method of the global QCD analysis [4] or, still limitedly, from a lattice QCD computation. The functional forms of PDFs are *a priori* unknown locally, while globally they satisfy several expectations such as sum rules and integrability of moments. Search for such functions by fitting them to cross section data has been tackled within two main paradigms: either inferring parameters of user-constructed fixed parametrization forms or using neural networks. Proton and other PDFs, so determined, are then used to predict further observables and extract Standard Model parameters. Their role in precision physics is of the utmost importance. It is why the leading groups that determine the most precise proton PDFs [5–7] joined their efforts in a benchmarking and combination exercise to provide PDFs for the high-luminosity LHC era [8]. Further progress towards comprehensive NNLO and N3LO PDFs has been achieved recently by several groups [9–13].

As we strive for ever-increasing precision and accuracy of PDFs, it is essential to account for all leading sources of their uncertainty. Among these, quantifying the important epistemic uncertainty due to the PDF parametrization poses a special challenge in light of the vast number of possible realizations as well as subtle, yet consequential biases that may affect the analysis [14]. This viewpoint, and the critical effort that it implies, has been adopted and refined in further AI/ML-oriented studies [15–18]. Assigning a probability distribution to the epistemic uncertainty focuses on the representativeness of the sampling of the solutions for PDFs [14, 19–21].

Fantômas is a C++ package to parametrize PDFs, or x -dependent nonperturbative correlator functions in general, with the help of Bézier curves – representations for arbitrary polynomials defined in a universal Bernstein basis. Bézier curves here refer to 1-dimensional polynomials $f(x)$ whose coefficients are computed from the values $f(x_i)$ at several control points x_i specified by the user. According to the Stone-Weierstrass theorem – a classical universal approximation theorem akin to the ones [22–24] that justify neural networks – for any continuous differentiable function of x , there is a Bézier curve that approximates this function to the desired accuracy. Such polynomial approximators offer advantages compared to neural-network models, such as low dimensionality of the parameter space and transparent interpretation. By constructing the polynomials from their values at control points, instead of fitting the polynomial coefficients directly, one gains a certain leverage over the interpolation or fitting procedure, as explored in this article.

The capabilities of the Fantômas framework were first demonstrated in a fit of pion PDFs [25, 26], yielding significant physics insights. The pion PDFs are less known than the nucleon ones. Previous modern analyses of the PDFs in the pion [27–29] displayed narrow uncertainty bands in spite of the paucity of data in the intermediate x region and large uncertainty at small x . We implemented the Fantômas parametrizations in the xFitter fitting framework [30], which was used for one such earlier fit [28], and performed a comprehensive analysis of the parametrization dependence by generating about 100 fits with varied Bézier parametrizations. In these fits, the degree of a polynomial was raised simply by adding a new control point to the parametrization available from a previous fit. These and other features streamlined generation of distinct fits, which were then combined into a single uncertainty band using the METAPDF combination method [31]. The uncertainty from the nuclear PDFs was added in the final release of FantoPDF PDFs [26]. This was the first set of pion distribution functions to comprehensively account for the parametrization uncertainty, achieving notable agreement with lattice QCD determinations of the pion PDFs. A key finding was that the large- x experimental data constrains the valence PDF, whose fixed-order perturbative behavior is consistent across fitting groups. In contrast, the sea and gluon PDFs are anti-correlated and remain challenging to disentangle due to the limited data available at small x .

The Fantômas toolkit is shared on our git repository in two versions. First, a standalone version demonstrates core features of the Fantômas methodology on simple examples and does not have any significant external dependencies. The xFitter version is built as an extension of the public xFitter code. Specifically, we exploited the modular structure of xFitter 2.2.0 to integrate the Fantômas components by adding a section in the module with PDF parametrizations.

As a validation example, in the `xFitter` version we included a short fit of the pion PDFs from our baseline analysis in [25]. Both versions will be described hereafter. In this paper, as in Ref. [25], we have illustrated the functionality of `Fantômas` using a toy model in `Mathematica` (available by request) and the `xFitter` set-up for the pion PDF fit [28], hence addressing both simple and real physics-case scenarios.

The paper is structured as follows. The core of the problem we confront through `Fantômas`, namely the role of parametrizations in global analyses, is motivated in Section 2. The mathematical concept behind the metamorph solution to this problem, as well as first-principle constraints on PDFs, are spelled out in that same Section. The `Fantômas` toolkit is fully detailed in Section 3, where we discuss the main code base: classes, core source files, and steering cards, along with several examples. This section also includes the inputs and outputs, as well as the various options to activate the metamorph, such as the nature of the control points. Then, both the standalone version and the `xFitter` implementation are discussed. We then illustrate in Section 4 how to use `Fantômas` in the context of pion PDF fits. This includes a step-by-step procedure (Section 4.1) for generating the fits; a dissection (Section 4.2) of the resulting ensemble of analyses intended to illustrate the behavior of `Fantômas`; and an exploration (Section 4.3) of the full power of metamorph through guidelines on tuning the flexibility of the parametrization(s). Knowing the full power of the metamorph, we discuss the combination of PDFs from various parametrizations as well as with further, uncorrelated, uncertainties in Section 5. After summarizing the “do’s and don’t’s” in Section 6, we draw our conclusions in Section 7. The various Appendices offer more details on technical aspects of the code and its performance, from a brief review of the `xFitter` environment (Appendix A), to a discussion (Appendix B) on numerical artifacts pertaining to the pion fits of Section 4, as well as a sample `Mathematica` notebook (Appendix C).

2. Functional forms for PDFs

2.1. The role of parametrization studies in modern PDF fits

In various inverse problems arising in global analyses of hadron structure, the inference of unknown functions quantifying non-perturbative QCD dynamics starts by choosing a convenient (non)parametric representation, which must be differentiable and satisfy certain physics limits. This representation is then constrained by a fit to discrete data. Among the various representations, polynomial functions and neural networks (NNs) are most commonly used and have reached the highest level of sophistication in QCD analyses of unpolarized PDFs.

In practice, modern PDF fits must continually revisit the question of the parametric flexibility which is needed in order to adequately model an ever-expanding global set of hadronic data. Global fits based on explicit, analytical parametrizations typically operate with polynomial-based functional forms with 5-10 parameters per flavor, mirroring the adaptive nature of [trained and cross-validated] NNs. Meanwhile, NN-based fits must similarly confront their inherent parametrization dependence as realized through their chosen number of nodes, hidden layers, and overall network topology. Addressing these challenges in a systematic fashion requires the nontrivial exploration of a wide array of parametrization forms and hyperparameters. The need for quantifying this parametrization dependence derives from the fact that the effect of choosing an assumed functional forms for analytical parametrizations or, equivalently, the architecture and training of a NN, can be substantial in precision PDF fits to large data sets, contributing together with other sources [Sec. 1G in 2] to the total PDF uncertainty.

Within this context, the `Fantômas` methodology we present in this manuscript streamlines the generation and fitting of versatile polynomial functional forms, thereby further narrowing the performance gap between these two standard approaches to parametrization in PDF analyses while supplying a novel approach for the fast generation of many explicit fitting forms. Polynomial parametrizations are appealing in that, while they are able to approximate arbitrary well-behaving functions, they have low complexity and are amenable to algebraic derivation from various predictions using methods of classical statistics, approximation theory, or the nonperturbative modeling of hadron structure. When we fit such a parametrization, we generally expect a tradeoff between the low agreement with the data, when the parametrization is too inflexible, and loss of the generalization power when the parametrization is too flexible and responsive to the stochastic noise in the data. Training of neural networks often employs cross validation to obtain a PDF model that reasonably balances between these two extremes. The point of the balance can be approximately determined, *e.g.*, by controlling the bias-to-variance ratio [9] in either the analytical or NN approach.

That said, a large volume of data does not imply a unique PDF model or full suppression of the parametrization uncertainty. As a matter of fact, functional forms for PDFs cannot be uniquely determined solely based on discrete

experimental measurements because of the mathematical property of PDF parameterization mimicry [32], which is enhanced in the regions of scarce data coverage, known as extrapolation regions. The non-uniqueness of the best-fit solution can be demonstrated first by interpolating or fitting data with a polynomial approximator and applying the unisolvence theorem [32], and then showing that the result extends to other types of universal approximators, which themselves can be approximated by some polynomial to a given accuracy.

A closure test of a given fitting methodology [9, 33], verifying an excellent agreement between the best-fit PDF solution and the known “truth PDF” used to generate the fitted pseudodata, does not generally preclude existence of multiple functional forms achieving comparable agreement with the discrete data when such “truth” is *a priori* unknown. In the Bayesian paradigm, one must initially assume an uninformed prior when trying equally plausible PDF functional forms. The combined posterior prediction based on the totality of explored functional forms can then be constructed using several available methods, such as Bayesian model averaging [19, 34] or discrete profiling [35]. All such studies run into a serious challenge of representative and unbiased exploration (sampling) of large parametric spaces for PDFs [14] in order to minimize the distributional (miscoverage) component of the epistemic uncertainty [15–17, 36]. Such exploration is systematized through the use of Bézier curves to generate various parametrizations on the fly [25].

2.2. Metamorph

The methodology of Fantômas is based on the use of analytical forms called *metamorphs* to represent functions of a variable x defined over a supported region, $x \in [0, 1]$. In the context of PDFs, such functions represent the distribution, $f_a(x, Q_0^2)$, of a parent hadron’s fractional momentum, x , carried by a constituent parton of flavor, a , at an starting scale, Q_0^2 , of the Dokshitzer-Gribov-Lipatov-Altarelli-Parisi (DGLAP) evolution. This Section describes the mathematics behind the metamorph approach, while subsequent illustrations will be given throughout the article.

PDFs must follow, at small and large x , physically-motivated constraints and analyticity. To accommodate for such end-point behaviors, we parametrize the PDF as

$$xf_a(x, Q_0^2) = F_a^{car}(x) \times F_a^{mod}(x) \quad (1)$$

for each parton flavor a contributing at scale Q_0 . The “baseline” of our functional form is called the *carrier function*, F_a^{car} . The carrier function serves as the simplest parameterization form consistent with the above-mentioned constraints, particularly under the scenario $F_a^{mod}(x) = 1$. We have chosen to define our carrier function as

$$F_a^{car}(x) \equiv A_a x^{B_a} (1-x)^{C_a}. \quad (2)$$

Some normalization coefficients, A_a , are chosen to satisfy the flavor number and momentum sum rules; the other remain as free parameters of the fit. B_a and C_a govern the behavior of the parametrization under the limits $x \rightarrow 0$ and 1. Conceptually, the purpose of the carrier is to implement expectations for the x behavior following from the first principles or semi-qualitative models.

In Eq. (1), F_a^{mod} is the *modulator function*. The modulator allows more freedom at x away from 0 or 1. The modulator, expressed as $F_a^{mod}(x; \mathcal{B}^{(N_m)})$, is defined to be a function of $\mathcal{B}^{(N_m)}(y)$, a polynomial of order N_m and argument $y \equiv y(x)$, where $y(x)$ is a *stretching function*. In the simplest realization, $y(x) = x$. However, it can be any function of

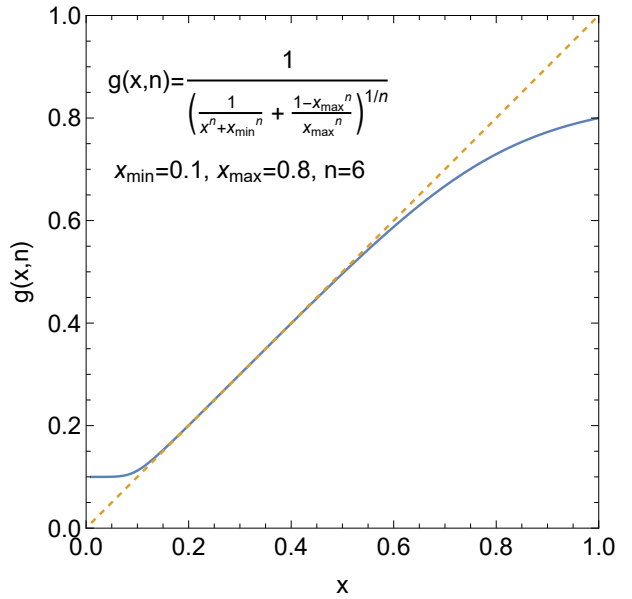


Figure 1: Plot of the stretching function $g(x, n)$ in Eq. (4) for $x_{\min} = 0.1$, $x_{\max} = 0.8$, $n = 6$. The dashed curve indicates the dependence $y = x$.

x . As an example, in the pion study [25], the modulator and stretching function are defined as

$$F_a^{mod}(x; \mathcal{B}^{(N_m)}) = 1 + \mathcal{B}^{(N_m)}(y), \quad (3)$$

and

$$y = (g(x, n))^{\alpha_x} \equiv \left(\frac{1}{\left(\frac{1}{x^n + x_{\min}^n} + \frac{1 - x_{\max}^n}{x_{\max}^n} \right)^{1/n}} \right)^{\alpha_x}, \quad (4)$$

with $0 < \alpha_x < 1$ and $n = 6$ [25], as illustrated in Fig. 1. The function $g(x, n)$ freezes the x dependence below x_{\min} and above x_{\max} , where both x_{\min} and x_{\max} lie in the extrapolation regions of x (outside of the range covered by the data). In other words,

$$\lim_{x \ll x_{\min}} g(x, n) = x_{\min}, \quad \lim_{x \gg x_{\max}} g(x, n) = x_{\max}, \quad (5)$$

i.e., the asymptotic behavior of the whole metamorph $xf_a(x, Q_0^2)$ is controlled by the carrier $F_a^{car}(x)$ in these asymptotic limits. Fantômas automatically sets x_{\min} , x_{\max} according to the mandatory fixed control points, as described in Sec. 4.1. The power n determines the steepness of the freezout transition at $x \sim x_{\min}$ and $x \sim x_{\max}$. In between x_{\min} and x_{\max} , $g(x, n) \approx x$, cf. Fig. 1, so that $y \approx x^{\alpha_x}$. Hence, in the x region covered by the data, the argument of the Bézier curve is essentially x^{α_x} , where commonly used parametrizations take $\alpha_x = 0.5, 1$, or another positive fractional value.

In our methodology, the \mathcal{B} polynomial is chosen to be a Bézier curve,

$$\mathcal{B}^{(N_m)}(y) \equiv \sum_{k=0}^{N_m} c_k B_{N_m, k}(y) \quad (6)$$

by introducing a basis of Bernstein polynomials,

$$B_{N_m, k}(y) \equiv \binom{N_m}{k} y^k (1 - y)^{N_m - k}, \quad (7)$$

where the $\binom{N_m}{k}$ is a binomial coefficient. The Bernstein polynomials are neither orthogonal nor oscillatory. For a fixed degree N_m and index $k \in \{0, 1, \dots, N_m\}$, the Bernstein basis polynomial $B_{N_m, k}(y)$ attains its unique global maximum at $y_{(k)} = k/N_m$. Thus, the choice of the stretching function $y(x)$ controls spacing of the peaks $y_{(k)}$ of the Bernstein polynomials over $x \in [0, 1]$.

With the Bézier curve, the numerical coefficients c_k in Eq. (6) are not fitted directly; instead, they are calculated from the values of the modulator function $F_a^{mod}(x_i; \mathcal{B}^{(N_m)})$ at $N_m + 1$ distinct points x_i in the interval $x \in [0, 1]$, called *control points* (CPs). In the C++ code, class `ControlPoint` refers to a pair of real numbers $\{x, \mathcal{B}^{(N_m)}(y(x))\}$ specifying the x position (fixed during the fit) and the corresponding Bézier value, which can be a free parameter, for every CP. Hence, in contrast to traditional parametrizations used by PDF fits, the free parameters controlling the modulator are the values of the Bézier curve, *i.e.*, effectively the modulator $F_a^{mod} = 1 + \mathcal{B}^{(N_m)}$, at user-specified CPs.

Denote $P_i \equiv \mathcal{B}^{(N_m)}(y(x_i))$ at a control point x_i . We will solve for c_k in terms of P_i a matrix form [37, 38], denoting a scalar, an $(N_m + 1)$ -dimensional vector, and an $(N_m + 1) \times (N_m + 1)$ matrix as S (no underline), \underline{V} , and \underline{M} , respectively. We use Einstein's summation with Roman indices taking values between 0 and N_m . The unisolvence theorem for polynomials guarantees existence of a unique solution for c_k under the assumption that the Vandermonde matrix T defined below is invertible.

Given the vector $1, y, y^2, \dots, y^{N_m}$ containing incrementing integer powers y^p as $\underline{Y}(y)$, the vector of $\mathcal{B}^{(N_m)}(y_i)$ at $(N_m + 1)$ CPs $y_i \equiv y(x_i)$ as \underline{P} , and the vector of the Bernstein polynomial coefficients c_k as \underline{C} , we can show that our Bézier curve $\mathcal{B}^{(N_m)}(y) \equiv \mathcal{B}$ in Eq. (6) assumes the form

$$\mathcal{B} = \underline{Y}^T(y) \cdot \underline{M} \cdot \underline{C}, \quad (8)$$

where $\underline{\underline{M}}$ is an $(N_m + 1) \times (N_m + 1)$ matrix containing combinations of binomial coefficients,

$$\underline{\underline{M}} \equiv \|m_{lp}\| \text{ with } m_{lp} = \begin{cases} (-1)^{p-l} \binom{l}{n} \binom{n-p}{n-l}, & l \leq p \\ 0, & l > p \end{cases}. \quad (9)$$

From Eq. 8, we can represent \underline{P} as

$$\underline{P} = \underline{T} \cdot \underline{\underline{M}} \cdot \underline{C} \quad (10)$$

by introducing the Vandermonde matrix $\underline{T} \equiv \|Y_k(y_i)\|$ with $Y_k(y_i) = (y_i)^k$ (y_i raised to power k). Since under our assumptions it is a non-singular square matrix, we can invert this equation to obtain vector \underline{C} of Bézier coefficients as a function of CPs,

$$\underline{C} = \underline{\underline{M}}^{-1} \cdot \underline{T}^{-1} \cdot \underline{P}. \quad (11)$$

Once \underline{C} is found, we reconstruct the modulator $F_a^{mod}(x; \mathcal{B}^{(N_m)})$ at any $x \in [0, 1]$ using Eqs. (3) and (8), and then the complete metamorph $x f_a(x, Q_0^2)$ in Eq. (1).

The Bézier curve calls for the inversion of matrix \underline{T} in Eq. (11), which requires some care, especially at high N_m . Appendix B discusses the optimal placement of CPs that leads to stable inversion.

Many polynomial parametrizations used in PDF global analyses can be cast into the metamorph form simply by recomputing their numerical coefficients (without refitting). It is the case for the parametrizations utilizing the Bernstein basis used by CT, as well as the Chebyshev basis used by MSHT. While the neural networks of NNPDF are employed in a conceptually different manner, they could still be linked to polynomial approximators, given the smoothness of respective PDF solutions.

2.3. Sum rules and prior constraints

The form of a metamorph is usually constrained by global considerations such as sum rules and prior probabilities. In the current Fantômas toolkit, we implemented support for two main sum rules imposed on the unpolarized PDFs – the valence and the momentum sum rules, related, respectively, to the 0^{th} and the 1^{st} Mellin moment,

$$\langle x^n f_a \rangle(Q^2) = \int_0^1 x^n f_a(x, Q^2), \quad (12)$$

with q representing the flavors or flavor combinations, e.g., $q = \{V, S, g\}$ for a pion target [25, 28]. To uphold the sum rules in a given decomposition, the first moments need to be obtained through numerical integration. These sum rules usually dictate the value of the normalization for one metamorph function each. For example, in the pion study [25], the two sum rules to be fulfilled are

$$\langle V \rangle = 2, \quad (13)$$

and the momentum sum rule,

$$\langle xV \rangle + \langle xS \rangle + \langle xg \rangle = 1. \quad (14)$$

The `metamorph` class `Fantômas` provides a method `GetMellinMoment` to compute arbitrary Mellin moments at scale Q_0 by numerical integration. As a byproduct, the method tests for integrability of the metamorph function given its numerical parameters. Other prior constraints are related to analyticity of PDFs, smoothness and positivity (of cross sections). The latter can be tracked through prior penalties on the value ranges of specific parameters, as will be made explicit in Section 3.6.2.

3. The Fantômas toolkit

The Fantômas toolkit described in this Section provides a C++ implementation of metamorph parametrizations for PDFs detailed in Sec. 2. It also includes a wrapper in C that facilitates compilation with Fortran programs such as xFitter.

We review the classes of the Fantômas toolkit in Sec. 3.1; core files, inputs, and outputs in Sec. 3.2, including an example of the steering card in Sec. 3.2.1; the fitting algorithm in Sec. 3.3; the C wrapper functions in Sec. 3.4; the standalone implementation in Sec. 3.5; and the xFitter implementation in Sec. 3.6.

3.1. Classes

Fantômas defines the following classes:

1. Class `ControlPoint` defines a control point at position x , with the value of the function at this point accessed via a pointer `*ps`.
2. Class `metamorph` implements a PDF parametrization for a single flavor according to Eq. (1) in the form

$$xf(x) = \text{Carrier}(x, Sc) * \text{Modulator}(x, Sm),$$

where `Carrier` defines the asymptotic behavior in the limits $x \rightarrow 0$ and $x \rightarrow 1$; `Modulator` determines the behavior of $f(x)$ over the interval $0 < x < 1$. Parameters of the `Carrier` and `Modulator` are respectively stored in external arrays `Sc`, containing A_a, B_a, C_a in Eq. (2), and `Sm` with values of P_i . Internally, `Modulator(x, Sm)` is controlled by a private vector of Bézier coefficients \underline{C} . Every time when the fit updates the CP values P_i , i.e., $F^{mod}(x_i) - 1$, Fantômas must recompute \underline{C} by calling `metamorph::UpdateModulator()`.

The `metamorph` class provides the following public methods:

- `double metamorph::f(const double x)` returns the value of the metamorph for the momentum fraction x .
 - `void metamorph::UpdateModulator()` computes vector \underline{C} of Bézier coefficients using Eq. (11). This computation must be done every time after the control points (i.e., the array `Sm[]`) are updated, and before the metamorph value f is computed.
 - `double metamorph::Modulator(const double x)` returns the value of the Modulator function for the momentum fraction x .
 - `double metamorph::yx(const double x)` returns the stretched argument $y(x)$ of the Bézier curve.
 - `void metamorph::SetXstretching()` and `void metamorph::GetXstretching()` set and return parameters of the stretching function $y(x)$.
 - `double metamorph::GetMellinMoment(double MellinPower, int npts = 10000)` returns $\langle x^{n+1} f_a \rangle$, with $n = \text{MellinPower}$, i.e., the $(n+1)$ -th Mellin moment over $0 \leq x \leq 1$. This prescription for orders of Mellin moments follows the one adopted in xFitter. `npts` is the number of points for Gaussian integration over x . By default, `npts=10,000`.
 - `double metamorph::Cs(const int i)` returns the value for the i -th Bézier coefficient.
 - `double metamorph::GetConditionNumber()` returns the condition number of matrices T and T^{-1} using the Frobenius norm, $\|T\|$, i.e., the square root of the sum of absolute squares of the elements. The condition number is calculated as $\|T\| \cdot \|T^{-1}\|$. See Appendix B.
 - `double metamorph::chi2prior()` returns a contribution to χ^2 from the prior imposed on the metamorph
3. Class `metamorphCollection` is a container for `Nmeta` `metamorph` objects providing parametrizations for parton distributions of distinct flavors. `metamorphCollection` also provides methods to read, update, and return parameters and PDF values for a `metamorph` object corresponding to a physical flavor ID `ifl`, such as the PDF flavor assignment according to the LHAPDF convention. The physical flavor ID is specified in the steering card, cf. Sec. 3.2.1, and matches the flavor assignment in the external fitting program.

Private members of `metamorphCollection` include:

- `vector<metamorph> MetaVector` contains `metamorph` objects in the `metamorphCollection`;

- `map<int, metamorph*> MetaRoster` maps the integer physical flavor `ifl` onto the pointer to the corresponding metamorph in `MetaVector`;
- `map<int, int> PositionRoster` maps the physical flavor `ifl` onto the integer position `iMet` of the corresponding metamorph in `MetaVector`.

The `metamorphCollection` class provides the following public methods:

- `void metamorphCollection::ReadCard()` reads input parameters (powers of the carrier, control points, etc.) for all metamorphs from an input steering card, see Sec. 3.2.1. Analogously, `metamorphCollection::WriteCard()` writes all parameters into a new steering card.
- `void metamorphCollection::UpdateParameters(const int ifl, double *deltas)` updates the metamorph for physical flavor `ifl` according to the provided changes `deltas` in the parameters. `UpdateModulator()` is called within this method.
- `double metamorphCollection::f(const int ifl, const double x)` returns the value of a metamorph with physical flavor `ifl` at momentum fraction `x`.
`metamorphCollection::MellinMoment` and `metamorphCollection::GetConditionNumber` respectively return a Mellin moment and condition number for the metamorph with physical flavor `ifl`.
- `int metamorphCollection::GetMetamorphCount()` returns the number of metamorph members in `MetaVector`.
- `double metamorphCollection::chi2prior()` returns a contribution to the objective function, χ^2 , from the sum of priors on all metamorphs
- `void metamorphCollection::MetamorphDiagnostics(const string& outputDirectory)` saves diagnostics about the metamorph collection into `fantomas_functional_parameters.txt` in a directory `outputDirectory`. The diagnostics includes values of carrier and modulator parameters, momentum fractions, and condition numbers. `void metamorphCollection::Chi2Diagnostics` saves the diagnostics about prior penalties. In `xFitter`, `outputDirectory = output/`.

3.2. The core source files, steering cards

The following **source files** and the respective C++ header (`.h`) files define the **Fantômas** classes and provide core functionalities:

1. `metamorph.cc` defines classes `ControlPoint` and `metamorph` for individual control points and metamorph parametrizations, respectively.
2. `metamorphCollection.cc` defines class `metamorphCollection`. A companion file `metamorphCollectionPrior.cc` contains definitions of the prior penalties on metamorphs that can be fit-specific and saved in `xFitter` together with the rest of the outputs.
3. `LUPinverse.cc` and `cl2DArray.h` support matrix operations, including inversion.
4. `FantoWrapper.cc` provides an extern "C" wrapper for the core **Fantômas** methods, see Sec. 3.4.

Steering cards play an important role in the **Fantômas** algorithm, in that they store metamorph parameters and settings in an extended format that is not normally supported by control cards in MINUIT or another fitting program. During the fitting, the output steering card saves the metamorph parameters that achieved the lowest χ^2 among all values explored. We set the MINUIT fitting parameters to correspond to the changes from the tabulated values in the steering card, see Sec. 3.3, which simplifies bookkeeping. **Fantômas** therefore operates with two steering cards:

- `steering_fantomas.txt`: an input file that contains the initial parameters – information about the control points, order of the Bézier curves, the mapping parameters– used to create the metamorph. This file is accessed by the `void metamorphCollection::ReadCard()` method.
- `steering_fantomas_out.txt`: this is a new steering card containing the updated metamorph parameters. It is created by calling `metamorphCollection::WriteCard()`. In the `xFitter` realization, this card is updated every time when a lower χ^2 is found.

3.2.1. Example of a steering card

The steering card stores parameters and settings for all metamorph functions. Figure 2 shows an example of such a card. Line 1 specifies the format version and should not be modified. The header with comments marked by “#” is followed by several blocks for input metamorphs, with each metamorph associated with its physical flavor ID `ifl` (according to the LHAPDF or another convention), by which this metamorph can be addressed from the external code via the respective method of `metamorphCollection`. For each such block, the settings are

$$\{N_m, \text{MappingMode}, \text{xPower} \equiv \alpha_x, \text{Sc}[0] \equiv A_a, \text{Sc}[1] \equiv B_a, \text{Sc}[2] \equiv C_a\}.$$

The first entry is the degree of the polynomial; the second is related to restricting the value of $f(x)$ to stay within constraints – the mapping mode. It is a placeholder for imposing bounds on the parametrization. Currently we only use `MappingMode` = 0, which does not impose constraints. The scaling factor `xPower` is defined in Eq. (4), and the array `Sc[]` contains the carrier’s parameters in Eq. (2). Then, the block contains $(N_m + 1)$ records with parameters for the metamorph’s CPs, $X_s \equiv x_i$ for the x positions, and `Sm[i]` for either P_i or the flag indicating a CP of a special type.

Specifically, the `Sm` column should contain one of the following four entries to select from:

- A real number (referred to as “FREE” in [25]): this is the initial $P_i = \mathcal{B}^{(N_m)}(y_i)$ value of the Bézier function used in the metamorph.⁷
- “FIX”: This option fixes $P_i = 0$, $F_a^{mod}(x_i) = 1$ for the rest of the fit, so that the metamorph *always* coincides with the carrier function at this CP. **We recommend to FIX the zeroth and last CPs, with x_0 and x_{N_m}** , in which case Fantômas sets $x_{\min} = x_0$, $x_{\max} = x_{N_m}$ in the stretching function $g(x, n)$ in Eq. (4). With this setting, $F^{mod} = 1$ at $x < x_0$ and $x > x_{N_m}$: the metamorph then coincides with the carrier $A_a x^{B_a} (1 - x)^{C_a}$ at $x \rightarrow 0$ or 1.
- “NEW”: This option will calculate P_i at this CP, x_i , by using a metamorph function of a lower order, *e.g.*, $N_m - 1$, specified solely by the rest of the provided control points.
Use the NEW option to add control points to the pre-existing modulator, hence raising the polynomial degree N_m without modifying the modulator’s initial shape or values at the already existing CPs.
- “CALC”: This option will calculate the P_i value at this CP when writing the output. This control point will not be used to calculate the metamorph function.

3.3. The fitting algorithm

The fitting in xFitter proceeds as follows. We create an input steering card, `steering_fantomas.txt`, containing the initial metamorph parameters. We also modify a MINUIT steering card to assign free parameters to the *changes* of the varied metamorph parameters. We call the latter the δ (delta-) parameters, such that $\{A_a, B_a, C_a, c_{l,i}\} \rightarrow \{A_a, B_a^0 + \delta B_a, C_a^0 + \delta C_a, c_{l,i}^0 + \delta c_{l,i}\}$, for all but the A ’s. Those A_a can either be determined by sum rules or let as free parameters. For example, out of the three normalizations of the pion PDFs, the valence normalization constant A_V is calculated following the valence sum rule,

$$A_V \int_0^1 f_{\text{meta}}^V(x) dx = \langle V \rangle \quad (15)$$

where f_{meta}^V is the output of the metamorph module.⁸ Either the sea normalization or the gluon normalization is varied independently, while the third normalization is computed to fulfill the momentum sum rule by subtraction, *e.g.*, at Q_0^2 ,

$$\langle xg \rangle [A_g(A_V, A_S)] = 1 - \langle xV \rangle [A_V] - \langle xS \rangle [A_S], \quad (16)$$

⁷We remind the reader that the full metamorph at a CP x_i is given by $F^{car}(x_i) \times (1 + P_i)$.

⁸Another way of enforcing the correct normalization relies on the analytical expression for the first moment. This has been used extensively in the past, and still adopted by the xFitter team in the pion study [28]. However, we chose to not forgo a constant in front of A_V to keep our metamorph function as general as possible, and to keep the parametrization linear in the parameters. Comparisons of both methods for the pion PDFs have been discussed in Ref. [25].

```

1 # Fantomas steering card v. 1.0cd
2 # YYYY-MM-DD HH:MM:SS
3 # gluon -- metamorph 0
4 # ifl Nm MappingMode xPower Sc(0) Sc(1) Sc(2)
5 0 0 0 1. 1. 0. 0.
6 # Xs Sm
7 0.7 FIX
8 # sea -- metamorph 1
9 # ifl Nm MappingMode xPower Sc(0) Sc(1) Sc(2)
10 1 3 0 1. 1. 1.02 9.14
11 # Xs Sm
12 0.001 FIX
13 0.4 0
14 0.7 0
15 0.8 FIX
16 # valence -- metamorph 2
17 # ifl Nm MappingMode xPower Sc(0) Sc(1) Sc(2)
18 2 3 0 1. 1. 0.73 0.95
19 # Xs Sm
20 0.01 FIX
21 0.4 0
22 0.7 0
23 0.999 FIX

```

Figure 2: An example of a Fantômas steering card, `steering_fantomas.txt`.

where we have made the dependence on the normalization explicit.

Hence, in the external fitting program, a delta parameter must be assigned to every free parameter of the metamorphs: `Sc[]` as well as `Sm[]` for *free* CPs. While the deltas for *FIXed* CPs are redundant and will be ignored by `metamorphCollection` even if assigned, the structure of the `xFitter` input nevertheless requires to assign the delta to the *FIXed* CPs as well. In the standalone MINUIT or other fitting programs, the deltas can be skipped for the *FIXed* CPs.

Within `parameters.yaml` of `xFitter`, all delta parameters are initialized with a zero value. They are updated as the fit progresses and passed into `metamorphCollection` to compute the current `Sm` and `Sc` parameters from the sum of the corresponding initial value and the delta. The final metamorph parameters corresponding to the lowest χ^2 are saved in `steering_fantomas_out.txt`. The final values of deltas are saved only in the diagnostic files, such as `minuit.out.txt`.

For example, for the change `delBv` in B_V in `xFitter` (parameter 7 in MINUIT), we assign in `parameters.yaml`:

```

1 Parameters:
2 ...
3 delBv: [ 0., 0.03]
4 ...
5 Parameterisations:
6   v:
7     class: Fantomas
8     parameters: [Av, delBv, delCv, delDv, delEv, vifl]
9 ...

```

The respective input printout in `MINUIT.out.txt` is

```

1  PARAMETER DEFINITIONS:
2  NO.   NAME      VALUE      STEP SIZE      LIMITS
3  ...
4  7 'delBv'      ' 0.0000    0.30000E-01    no limits
5  ...

```

The MINUIT output printout, which is only retained for diagnostics, is

```

1  ...
2  EXT  PARAMETER                                STEP      FIRST

```

3	NO.	NAME	VALUE	ERROR	SIZE	DERIVATIVE
4	...					
5	7	delBv	-0.30241	0.94832E-01	0.24034E-04	-0.14744E-03

The updated value of B_V is saved as `Sc[1]` for the valence metamorph in `steering_fantomas_out.txt`.

We can reuse `steering_fantomas_out.txt` as a steering card for subsequent fits and also to increase flexibility of the metamorphs in this card by adding one or more CPs to the metamorphs. For the latter, we increase N_m by the number of added CPs and insert these CPs as ``NEW" in the "Xs Sm" list. The advantage of this practice is that insertion of the NEW CPs does not quantitatively change the metamorph saved from the previous fit, as the new CPs are placed exactly on the old modulator. The χ^2 is exactly the same at the end of the previous fit and start of the new one, cf. an illustration in Fig. 5.

3.4. The C wrapper

To facilitate the interface of Fantômas with external codes, `FantoWrapper.cc` defines C functions invoking several core Fantômas functionalities. These functions are used to link Fantômas to the `xFitter` code as described below.

- `readfantosteer_()`: This function will read the card file, `steering_fantomas.txt`, by calling `ReadCard()`, and initialize a `metamorphCollection` for the metamorphs specified in the steering card. In `xFitter`, this function appears in the `atStart()` function in `Fantomas_PdfParam.cc` to ensure that the collection is created once.
- `writefantosteer_()`: The Fantômas module produces an output steering card by calling `WriteCard()` and, optionally, other output files. In `xFitter`, this function appears within `src/fcn.f` of the main `xFitter` source code, and is designed to update the output file to represent the fit with the lowest χ^2 encountered during the fitting process. This ensures that there are Fantômas outputs if the fitting process is halted before completion.
- `updatefantopars_(int &ifl, double pars)`: updates parameters of the metamorph with the physical flavor `ifl` using the deltas at pointer `pars`, i.e., it is a wrapper for the methods `UpdateParameters` and `UpdateMetamorphs` of `metamorphCollection`. `xFitter` will vary the parameters with each iteration. This requires `xFitter` to update the PDF values by calling `atIteration()`. The updated parameters are passed via the array of parameters from `xFitter`, `pars`. The module keeps track of which metamorph to use via the `flavor` argument.
- `fantopara_(int &ifl, double &x)` returns the numerical value of the metamorph for a given physical flavor `ifl` and `x` value. Within `xFitter`, this function is called when `operator(x)` is called.
- `fantoMellinMoment_(int &ifl, int &MellinPower, int npts)` calculates the $(n+1)$ -th Mellin moment, for $n = \text{MellinPower}$, physical flavor `ifl`, and `npts` integration points.
- `void getfantoChi2_(double& fantoChi2)` returns a contribution to the objective function (χ^2) from the prior constraints on metamorphs.

3.5. The standalone Fantômas implementation

The `standalone` directory of our Gitlab repository provides a lightweight implementation of the Fantômas toolkit and simple usage examples. The standalone code illustrates the generation of metamorph forms, updating the metamorph parameters using the deltas, computation of Mellin moments, and updating the steering card. The standalone implementation does not require a minimization package; implementation in `xFitter` will be described in Sec. 3.6.

`README.md` contains compilation instructions for the standalone examples. `FantomasExample_Cpp.cc` and `FantomasExample_Wrapper.cc` respectively provide a sample Fantômas run invoked directly in C++ and using the C wrapper from Sec. 3.4.

The C++ example first reads `steering_fantomas.txt` to create an instance `metacol` of the `metamorph-Collection` class for pion-like parametrizations: valence $xV(x)$, sea $xS(x)$, and gluon $xg(x)$. Recall that the `metamorph` collection stores all relevant information on the metamorph functions for all flavors and accesses individual metamorphs according to their physical flavor `ifl`. It also provides methods to update all metamorphs at once or retrieve information from them.

The executable `FantomasExample.Cpp.x` created upon the compilation demonstrates these multiple features that are encountered during the typical minimization and will be described in the next subsection. There is no minimization involved in the standalone version, but the example imitates updates of the metamorph parameters in the following way. `Fantômas` reads the initial metamorph parameters from `steering_fantomas.txt`, while the external fitting program computes their changes (deltas). Thus, as seen from the fitting program, the fitted parameters are the “deltas”, not the metamorph parameters themselves. The example simulates the updates in deltas by randomly varying them. It then adjusts normalizations of some PDF flavors to satisfy the valence and momentum sum rules. At the end, the example writes the updated metamorph parameters into `steering_fantomas.out.txt`.

The C++ example in `FantomasExample.Cpp.cc` proceeds as follows.

- It reads the steering card file `steering_fantomas.txt`, described at length in Section 3.2.1. If the printout of detailed diagnostics is requested (`VerbosityLevel=1`), it optionally prints out initial values of metamorph parameters, including `xPower`, `Sc[]`, and `Sm[]`. It then prints momentum fractions $\langle xf \rangle$, the values of the sum rules, and a table of PDF values vs. x .
- The next part of the code emulates the MINUIT interface in which the delta parameters are defined for relevant `Fantômas` parameters, `Sc[]` and `Sm[]`. The number of deltas should match the number of free parameters in all metamorphs, which requires manual editing of `FantomasExample.Cpp.cc` and can be automated in the actual fitting program.

In the example, we initialize the deltas for the overall normalization `Sc[0]` to 1 and the rest of the deltas to zero. We then shift the deltas by a random amount between 0 and 1, to simulate the real minimization, in which parameters are varied by arbitrary amounts to adapt to the data. We update the metamorphs using the deltas and recompute some normalizations to satisfy the sum rules. Values of `FIXed` points remain unchanged.

For instance, here is a part of the code that updates the gluon metamorph using a vector `deltag` containing the deltas.

```

1 // define the maximal orders of the metamorphs (number of CPs in
                                steering_fantomas.txt minus
                                1)
2 int Nmg = 3, NmS = 3, NmV = 3;
3 // define the total number of parameters
4 int ng = 6, nS = 7, nV = 7;
5 vector<double> deltag(ng + 1, 0.0); // length = ng+1
6 // set normalizations to 1 for all flavors
7 deltag[0] = 1;
8
9 //Generate random shifts
10 int seed=363432;
11 mt19937 gen(seed); // Mersenne Twister engine
12 uniform_real_distribution<> dis(0.0, 1.0); // Range [0, 1)
13 //Change deltas of the carrier...
14 for (int i = 1; i < 3; i++){
15     deltag[i] = dis(gen);
16 }
17
18 // ... and of the non-fixed CPs
19 for (int i = 0; i < Nmg; i++)
20     deltag[i+3] = dis(gen);
21
22 //Update the metamorph
23 metacol.UpdateParameters(iflg, deltag.data());
24 //Compute and print the momentum fraction
25 momg = metacol.MellinMoment(iflg, Mellinxf);

```

```

26 cout << "<xg> = " << momg << endl;
27 ...
28 //Updated the gluon normalization, provided momentum fractions
29 //for all three PDFs
30 // Ag*<xg> + AS*<xS> + AV*<xV> = 1
31 double Ag = (1 - momS - momV) / momg;
32 deltag[0] = Ag;
33 metacol.UpdateParameters(iflg, deltag.data());

```

The code prints out the current values of gluon parameters, deltas, and the momentum fractions before and after the metamorph normalizations:

```

1 The deltas (changes in the parameters) are:
2 deltag={1.000000e+00, 9.303177e-02, 6.096957e-01, 8.542143e-01, 5.737977e-01,
          2.180139e-01}
3 updated Scm[0][1] = 0.620432, deltas[1] = 0.093032
4 updated Scm[0][2] = 3.406296, deltas[2] = 0.609696
5 updated Scm[0][3] = 11.511414, deltas[3] = 0.854214
6 updated Scm[0][4] = 4.050728, deltas[4] = 0.573798
7 updated Scm[0][5] = 0.290044, deltas[5] = 0.218014
8 updated Scm[0][6] = 0.021282, deltas[6] = 0.000000
9 ...
10 Updated momentum fractions before normalization:
11 <xg> = 0.14764369
12 <xS> = 0.28907919
13 <xV> = 0.39470286
14 <V> = 1.59060336
15 total momentum: 0.83142574
16 ...
17 Momentum fractions after normalization:
18 <xg> = 0.21462756
19 <xS> = 0.28907919
20 <xV> = 0.49629325
21 <V> = 2.00000000
22 total momentum: 1.00000000

```

- At the end, the example saves `steering_fantomas_out.txt` with the updated metamorph parameters.

Finally, `FantomasExampleWrapper.x` realizes the same example in C, rather than C++, using the wrapper.

3.6. The xFitter implementation

3.6.1. Core files

The xFitter framework is reviewed in Appendix A. In the xFitter environment, the Fantômas toolkit implements a new parameterization of PDFs at the level of section “3) Theory” of the flowchart of Fig. A.9. Our main files, including the xFitter interface that descends from the 2020 pion fit [28], are deployed in directory `pdfparams/Fantomas/`. In the top-level CMake files and main xFitter source, we made a small number of changes tagged by the comment `#lk` or `clk` and included via a preprocessor directive `FANTOMAS_XFITTER`. The flag that turns the directive on, `-DFANTOMAS_XFITTER`, is enabled in the top-level `CMakeList.txt`. Finally, a new PDF flavor decomposition was required in `pdfdecomps/` for certain types of the pion fit.

In subdirectory `examples/Pion.Fantomas/`, we provided control files to perform a sample pion fit with the Fantômas parametrization. To run the sample fit, copy control files, including `steering_fantomas.txt`, into the top xFitter directory and run `bin/xfitter`. Upon successful completion within about 5 minutes, the fit returns the output files in `output/`. These files can be compared against the expected ones in `examples/Pion.Fantomas/output_correct/`.

We will now elaborate on these augmentations. The main directory of the package, `pdfparams/Fantomas/`, contains the core source for Fantômas (cf. Sec. 3.2) as well as

- `CMakeLists.txt`: a CMake file, containing locations and names of the source code to be compiled.

- `fantomas.cc` and `fantomas.h`: contain the Fantômas C wrapper (Sec. 3.4) adapted for xFitter.
- `Fantomas.PdfParam.cc` and `Fantomas.PDFParam.h`: realize the xFitter interface to Fantômas using the following functions:
 - `atStart()` is executed when the parameterization is called the first time. It initializes all necessary class objects and variables.
 - `atIteration()` is called every time the parameters are changed by MINUIT. It updates the modulator function with the new parameters.
 - `operator(double x)` returns the numerical value of the metamorph function for a given x value.
 - `moment(int N)` calculates the N -th moment; typically used to determine normalization according to the sum rules.

When the δ parameters are changed by xFitter, they are passed into our metamorph functions only by calling the `atIteration()` method. Every such call recalculates the metamorph functions using the updated parameters that were just provided. Similarly to the other parameterizations, `operator()` returns the overall PDF to the theory calculations within the xFitter program: again, it is valid only after `atIteration()` has already updated the metamorphs following the change of parameters. Likewise, `moment()` passes the N -th moment from the internal calculation inside Fantômas.

By the global nature of sum rules, they must be applied to the whole PDF function at once; hence some normalization constants are updated inside the interface file `Fantomas.PdfParam.cc` and not in the metamorph function. In the example of the momentum fraction calculations given by Eq. (16), A_S was taken to be a free parameter, determined by the minimization procedure, while A_g is found by subtraction to the momentum sum rule. However, numerical instabilities may arise when fitting very small or zero gluon PDFs, affecting the final result [25, 26]. To stabilize the fits with a small gluon, we had to consider A_g as a free parameter and compute A_S as a function of A_V and A_g . For this scenario, we have introduced a new flavor decomposition for the pion PDF in `pdfdecomps/SU3_(PositivePion-)gluon`, effective at the level of the sum rules. It has to be specified in the configuration file `parameters.yaml` under `Decompositions`:

```

1 Decompositions:
2   pion:
3     class: SU3_PositivePion_gluon
4     valence: v
5     sea: S
6     gluon: g

```

3.6.2. χ^2 penalties

In the Bayesian paradigm, an xFitter PDF fit maximizes the posterior probability $P(T|D)$, or equivalently it minimizes

$$\chi^2 = -2 \ln P(D|T) - 2 \ln P(T) \equiv \chi_{LL}^2 + \chi_{\text{prior}}^2 \quad (17)$$

consisting of the log-likelihood χ_{LL}^2 and χ_{prior}^2 arising from the prior probability on the model. In realistic physics scenarios, the choice of the terms on the right-hand side comes with some freedom and plays an important role. The objective function χ^2 is usually computed in the main source, *e.g.*, in a Fortran function `FCN` in `fcn.f` in xFitter, where it should not be modified heavily. Our realization compiles `FCN` with a directive `FANTOMAS_XFITTER` to compute χ_{LL}^2 and then add a prior penalty χ_{prior}^2 on the metamorphs retrieved by call `getfantochi2()`. The latter provides a C wrapper to a C++ method `metamorphCollection::Chi2prior()` defined in a short dedicated file `metamorphCollectionPrior.cc`. When the χ^2 value is reduced, `FCN` saves `steering.fantomas_out.txt`, containing the latest metamorph parameters, and `metamorphCollectionPrior.cc`, containing the prior that may change between the fits. Both files are saved in `output/`, so that the lowest attained χ^2 can be reproduced if the fit is interrupted or repeated.

The included `metamorphCollectionPrior.cc` provides a basic realization of `Chi2prior()` consisting of several blocks for common types of penalties that may be imposed, including

- lasso and ridge penalties on CP values, $\sum_{i=1}^{N_m+1} |P_i|$ and $\sum_{i=1}^{N_m+1} P_i^2$, respectively; these can be activated to constrain the total deviation of the modulator from unity, introducing rigidity to the modulator form.
- activation functions constraining the growth of a PDF-dependent quantity Y , including the (rectified linear unit) activation function $\text{ReLU}(Y) \equiv Y\theta(Y) = \max(0.0, Y)$, and logarithmic activation function $|\log(1 + |Y|)|$. Y can typically be a metamorph at some x , metamorph parameter, or Bernstein coefficient C .

By default, the blocks of penalties are commented out and can be uncommented as needed to assemble

$$\chi_{\text{prior}}^2 = \sum_j w_j \chi_j^2, \quad (18)$$

where χ_j^2 is the penalty from the j -th block included with weight w_j that is also specified inside `Chi2prior()`. Such priors may, *e.g.*, guide the gluon's fall-off moderately at large x , the modulator function to effectively subside to the carrier, or ensure integrability, *e.g.*, at very small x values, through limiting the allowed values of the B parameters.

On the last point of **integrability**, the flexibility of the metamorph functions may lead to non-convergence of lowest Mellin moments, which has to be addressed at the level of individual PDF parametrization classes and not in the `xFitter` main code. Each parameterization class within `xFitter` provides an integration method specifically for the said class. Integrability can be checked, *e.g.*, when enforcing the sum rules. Class `metamorph` does not enforce integrability on the metamorph and instead issues a warning message when the integrand is potentially non-integrable. The provided metamorph functions are regular except in the limits $x \rightarrow 0$ and $x \rightarrow 1$, and hence integrability can be checked based on the asymptotic powers B_a, C_a of the carrier for $xf(x)$ and the requested power n of the Mellin moment $\langle x^n f \rangle$. [Here B_a, C_a are the current, not initial values.] `metamorph::GetMellinMoment()` warns that the n -th moment is non-integrable if either $B_a + n \leq -1$ or $C_a \leq -1$. If either combination is between -1 and -0.93, it warns about slow convergence of the moment.

If the warning occurs, such solutions can be disfavored by including a prior contribution, $w \text{ReLU}(-B_a - n - 1)$ or $w \text{ReLU}(-C_a - 1)$. Analogous prior constraints can be imposed directly on the PDF values, *e.g.*, to enforce **positivity**. We encourage the use of such priors over that of the bounds on parameters provided by, *e.g.* MINUIT, to control the prior constraints.

3.6.3. More on inputs and outputs

The Fantômas steering card, `steering.fantomas.txt`, must be placed in the top `xFitter` directory. A few other standard files of the `xFitter` package are pertinent to the Fantômas-based fits:

- `parameters.yaml` is a steering file that defines physical flavor IDs and delta parameters passed into metamorphs, as it also serves as the control file for the MINUIT minimization. The flavor ID and parameter assignments in this file must match the ones defined within `steering.fantomas.txt`. Appendix A summarizes the contents of `parameters.yaml` in the case of Fantômas fits, and it also lists other relevant input files.
- `output/MINUIT.out.txt` reports the status of the MINUIT minimization, including the final values of the delta parameters.
- `output/xFitterPi/` is an existing `xFitter` output directory containing produced LHAPDF grids (`xFitterPi_XXXX.dat` and `xFitterPi.info`).⁹

Finally, we note that a fit can simultaneously deploy Fantômas and non-Fantômas parametrizations, depending on the specific hadron and flavor. For example, in the pion fit we simultaneously use the Fantômas parametrizations for pion PDFs and LHAPDF parametrizations for nuclear PDFs. In such situation, the code runs additional checks to initialize both metamorph and non-metamorph functions.

⁹For the users who are not familiar with the LHAPDF format of <https://www.lhapdf.org/>, a Mathematica package that reads the grids, `ManeParse`, is available here: <https://ncteq.hepforge.org/mma/index.html>.

4. Practical example: pion PDFs

To illustrate the possibilities at hand when using the Fantômas toolkit, we go back to the fits of PDFs for charged pions [25, 26], consisting of the valence $xV(x)$ [$u - \bar{u} = \bar{d} - d = V/2$ in π^+], SU(3)-symmetric sea $xS(x)$, and gluon $xg(x)$ distributions. **The parametrization in Eq. (1), together with Eq. (3), is designed to progressively increase the flexibility of the PDFs, by first realizing the asymptotic behaviors with the carrier and adding control points providing modulation at mid- x values. The χ^2 decreases without interruptions under this procedure, as illustrated in an example in Fig. 5.** This section is centered around this example. It shows how to construct a family of metamorph parametrization starting from the carriers, then incrementing the flexibility of functional forms while introducing prior penalties to moderate unconstrained behavior of PDFs if the data are limited.

The data sets used for the pion PDF fit include three different processes – pion-induced Drell-Yan, prompt photon and leading-neutron DIS – for a total of 408 data points, with ranges in $x_\pi \in [\approx 10^{-3}, \approx 1]$ and $Q^2 \in [\approx 7, \approx 250]$ GeV. Previous studies (Refs. [25, 27]) have already emphasized the sparse coverage in the low- and mid- x regions. Even with the addition of the leading-neutron data, the mid- x , small- Q^2 region remains unpopulated, effectively making it an extrapolation region. This paucity of the pion data should be kept in mind, as it requires to introduce prior constraints in several cases to guarantee convergence of the fits.

In some presented examples, we introduce the penalties defined in Sec. 3.6.2 and with the activation functions and weights listed in Table 1. The AbsLog and ReLU I penalties both favor Bernstein coefficients $|c_l|$ of order $\mathcal{O}(1)$; in the examples, we impose such a penalty on all three flavors. The rest of the penalties disfavor some unphysical solutions for PDFs that are allowed due to the scarcity of the pion data. ReLU II favors a positive valence PDF at mid- to large- x values, while ReLU III disfavors a gluon PDF that falls off too rapidly, as $(1-x)^{C_g}$ with $C_g > 10$, at $x \rightarrow 1$. Penalties II and III call the PDFs at a given x and Q_0 .

Fig. 3 shows the AbsLog and ReLU penalties with $w = 1$ and 0.2 . While the $|\ln(1 + |C|)|$ (AbsLog) penalty “softly” turns on and disfavors large C values, the $\text{ReLU}(C - C_0)$ is more abrupt in that it is absent for $C < C_0$ and rapidly grows for $C > C_0$. Therefore, the ReLU penalty does not affect the fit at all as long as C is moderate. Such priors may, *e.g.*, guide the gluon to fall off moderately at large x , force the modulator function to effectively subside relative to the carrier, or ensure integrability as $x \rightarrow 0$ by limiting the allowed values of the B parameters. Other priors can be imposed, in addition to the ones listed, offering some advantages over the bounds on parameters provided, *e.g.*, by MINUIT.

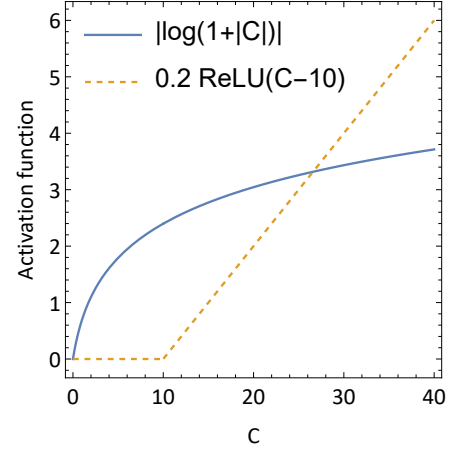


Figure 3: Activation functions listed in Table 1, with indicated weights.

Penalty name	Activation function	Weight w
AbsLog	$ \log(1 + c_l) $	1
ReLU I	$\text{ReLU}[c_l - 10]$	$1/(N_m + 1)$
ReLU II	$\text{ReLU}[\bar{u}(x, Q_0) - u(x, Q_0)], x = 0.1$	50
ReLU III	$\text{ReLU}[C_g - 10]$	50

Table 1: Penalties imposed for π^- PDF determination.

4.1. Building up a metamorph

A carrier-like metamorph. When building the parametrizations from scratch, the simplest metamorph is given by a carrier function multiplied by an $N_m = 1$ modulator $F^{mod} = 1$ with two fixed CPs set at the lower and upper ends, denoted by x_{\min} and x_{\max} , of the x region covered by the experimental data. Recall from Eq. (4) that the modulator’s

```

1 # gluon -- metamorph 0
2 # ifl Nm MappingMode xPower Sc(0) Sc(1) Sc(2)
3   0 1 0 1. 0.42 -0.37 2.83
4 # Xs Sm
5 0.001 FIX
6 0.8 FIX
7 # sea -- metamorph 1
8 # ifl Nm MappingMode xPower Sc(0) Sc(1) Sc(2)
9   1 1 0 1. 9.79 0.73 8.19
10 # Xs Sm
11 0.001 FIX
12 0.8 FIX
13 # valence -- metamorph 2
14 # ifl Nm MappingMode xPower Sc(0) Sc(1) Sc(2)
15   2 1 0 1. 2.54 0.74 0.95
16 # Xs Sm
17 0.001 FIX
18 0.8 FIX
19

```

(a)

```

1 # gluon -- metamorph 0
2 # ifl Nm MappingMode xPower Sc(0) Sc(1) Sc(2)
3   0 2 0 1. 0.42 -0.37 2.83
4 # Xs Sm
5 0.001 FIX
6 0.4 NEW
7 0.8 FIX
8 # sea -- metamorph 1
9 # ifl Nm MappingMode xPower Sc(0) Sc(1) Sc(2)
10   1 2 0 1. 9.79 0.73 8.19
11 # Xs Sm
12 0.001 FIX
13 0.4 NEW
14 0.8 FIX
15 # valence -- metamorph 2
16 # ifl Nm MappingMode xPower Sc(0) Sc(1) Sc(2)
17   2 2 0 1. 2.54 0.74 0.95
18 # Xs Sm
19 0.001 FIX
20 0.4 NEW
21 0.8 FIX

```

(b)

Figure 4: Initial steering cards for (a) the simplest $N_m = 1$ fit with 2 FIXed CPs and (b) an extended fit with 2 FIXed, 1 FREE CPs per flavor.

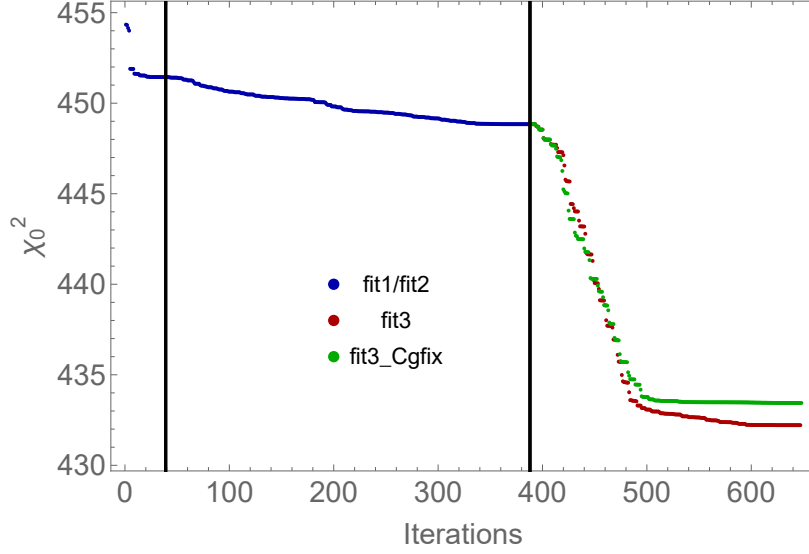


Figure 5: Illustration of χ_0^2 , the lowest χ^2 value when an improvement is detected in the fitting process, which decreases when adding CPs. The number of iterations is accumulated for the three fits (fit1, fit2, and either fit3 or fit3_Cgfix) corresponding to the addition of CPs, as the starting point for each higher degree polynomial comes from the best fit of the previous. See text.

argument is given by a stretching function $y(x) = g(x, n)^{\alpha_x}$, where $g(x, n)$ freezes the x dependence below x_{min} as well as above x_{max} . If the lowest (highest) CP is FIXEd, its x value sets the value x_{min} (x_{max}). With the two fixed CPs, $F_{mod} = 1$. Hence, the $N_m + 1 = 2$ control points translate into $c_{0,1} = 0$, leading to an effective $N_m^{eff} = 0$ metamorph.

One free control point. Figure 4(a) shows a sample steering card for such fit, called “fit1” in the following. Contrast this with another steering card for “fit2” in Fig. 4(b), in which we elevated degree N_m to 2 (by one unit) in lines 3, 10, and 17, and accordingly added NEW CPs in lines 6, 13, and 20. The NEW CPs are initialized with $P_i = 0$, so that they lie exactly on the parent metamorph. In the output steering card, the lines for these CPs contain their numerical P_i value instead of “NEW”.

Since the FIXEd CPs do not change their values, in general they do not require assignment of a free parameter for the respective deltas. In the xFitter realization, on the other hand, each CP requires an assignment of a delta parameter in `parameters.yaml`, but the values for the FIXEd CP’s can be left at zeros and will not change. We illustrate the respective record for the sea distribution in “fit2”:

```

1      Parameters:
2      ...
3          delDs: 0.
4          delEs: [ 0., 0.1]
5          delFs: 0.
6      ...
7      Parameterisations:
8      ...
9      S:
10         class: Fantomas
11         parameters: [As, delBs, delCs, delDs, delEs, delFs, sifl]
12     ...
13 
```

`delDs` and `delFs` stand for the free parameters for deltas of the CPs at $x = 0.001$ and $x = 0.8$. Their values (here set to 0. to comply with the xFitter internal convention) are ignored inside the metamorph. In the other fitting programs, specifying deltas for these FIXEd CPs would be redundant. The delta parameter `delEs` for the FREE CP at $x = 0.4$, however, has the initial value and initial step of 0. and 0.1, respectively. It corresponds to an active MINUIT parameter.

Two free control points. Once “fit2” converged, we add a NEW free CP to xV and to xS , raising N_m to 3 for these

Fit name	Free CPs	N_{par}	Penalty	χ^2	$\langle xg \rangle$	$\langle xS \rangle$	$\langle xV \rangle$
Main sequence							
fit1	{0,0,0}	7	ReLU	451.44	0.269	0.180	0.551
fit2	{1,1,1}	10	ReLU	448.84	0.257	0.187	0.556
fit3 (no convergence)	{1,2,2}	12	ReLU	432.61	0.120	0.448	0.432
fit3Cgfix (fixed C_g)	{1,2,2}	12	ReLU	433.43	0.130	0.427	0.443
Alternative fits							
fit2alt	{1,1,1}	10	AbsLog	451.18	0.269	0.180	0.551
fit1g	{0,0,0}	7	AbsLog	451.44	0.269	0.180	0.551
fit2g	{1,1,1}	10	AbsLog	451.18	0.269	0.180	0.551

Table 2: The NLO pion fits discussed in this section: name of the fit; numbers of free CPs in xg , xS , and xV ; number of free parameters N_{par} ; the penalty type; best-fit χ^2 values, and best-fit momentum fractions. The first four (last two) fits take the sea normalization A_S (the gluon normalization A_g) to be a free parameter. The χ^2 function includes both the log-likelihood and penalty contribution, as in Eq. (17). For two versions of fit2, small changes in χ^2 and momentum fractions reflect the differences between the AbsLog and ReLU penalties on Bernstein coefficients c_l .

flavors. We keep 1 FREE CP ($N_m = 2$) for the gluon, the least constrained PDF flavor. That is, our delta parameters for the CP's of xS are now `delCs`, `delDs`, `delEs`, `delFs`, `delGs`, with `delCs` and `delGs` for the two FIXED CPs now fixed at zero values. For a carrier-only setting “fit1”, each of the three flavor combinations had three free parameters, for a total of 9 parameters, two of which are determined by the valence sum rule and momentum sum rule. With five free CP's now at play, we have a total of 12 free parameters, which leads to flat directions in the PDF parameter space. We must constrain these directions either by fixing some parameters or adding prior penalties. In the following, we show results of such two fits, “fit3” and “fit3Cgfix”.

4.2. Exploring the pion fits

Dependence of χ^2 on the polynomial degree. The four just described fits, created by adding the free CPs as described, are listed as a “main sequence” in the upper half of Table 2 summarizing their settings. In this sequence, we uniformly apply the ReLU priors from Table 2 to guarantee the preferred physical behavior¹⁰ – but other solutions can be obtained by choosing the other priors or eliminating them entirely.

Figure 5 shows the dependence of χ^2 on the number of minimization iterations. The left Fig. 6 illustrates the variety of the PDF solutions obtained by increasing the polynomial degree, here visualized with the resulting gluon PDFs. Table 2 gives the resulting χ^2 and momentum fractions of the four fits.

Turning first to the χ^2 in Fig. 5, by adding the CPs to the solution of a converged fit, and hence increasing the degree of the polynomial of the modulator, we expect to see a decrease in the χ^2 value. In fact, the decrease happens with any polynomial parametrization, but only after all coefficients were refitted. With the common procedure that directly fits the polynomial (Bernstein) coefficients, the χ^2 initially increases after changing the polynomial's degree. This χ^2 increase does not happen with the metamorph parametrizations: when a new fit starts, addition of free CPs does not modify the progenitor metamorph function of a lower degree, and all Bernstein coefficients are recomputed accordingly. Hence, with the described procedure to increase the degree of the polynomial, the evaluated χ^2 initiates at an already low value found with the progenitor parametrization: we avoid cumbersome and redundant evaluations when the parametrization is changed.

This feature is illustrated in Fig. 5, where χ^2 remains continuous when we switch from fit1 to fit2 and then to fit3. The first iterations represent the optimization corresponding to fit1. The vertical lines show the initialization of the

¹⁰Penalty ReLU I is not activated in the carrier-only fit1, as all c_l 's are zero.

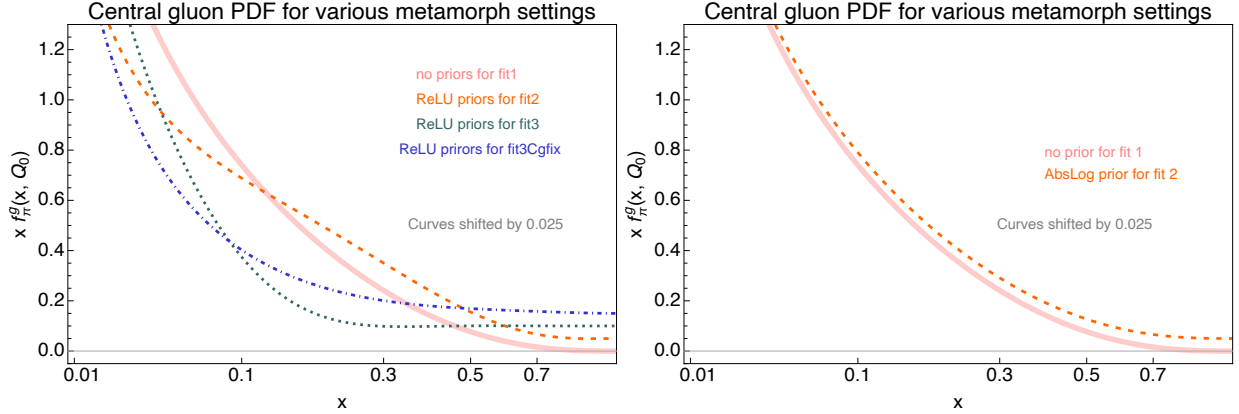


Figure 6: Central values for the gluon PDF of the pion using ReLU priors (left) and AbsLog priors (right), given at Q_0 , for the main sequence of fits Table 2. The consecutive curves have been shifted up by multiples of 0.025 for clarity. For fit1, neither of the described penalties have an effect.

following step, *i.e.*, fit2 or fit3. The χ^2 starts at the exact same minimum value as that found in the last iteration of previous step of the procedure.

Two versions of fit3 are illustrated, representing a baseline and a modified version of the same settings. For the sea and the valence, fit3 uses four CPs for each, with two CP's FIXED at the end points. The gluon PDF is kept at a lower order with only one free CP. With the fit settings in Table 1, fit3 does not converge – the data do not allow for two extra parameters to be determined. It is illustrated by the red dots in Fig. 5. When fixing the large- x behavior of the gluon to the best-fit value of the previous step ($\delta C_g = 0$), fit3Cgfix converges and the χ^2 reaches a plateau at a slightly higher value than fit3, shown by the green dots.

Figure 6 shows that the shape of the gluon PDF changes significantly as we progress through the sequence of four fits. Clearly, the order of the polynomial approximation matters for the PDF's behavior. In addition, the fits with at least one free CP (fit2 and fit3) are sensitive to the choice of the prior, as we illustrate by comparing the left and right panels of Fig. 6, obtained with the ReLU and AbsLog priors in Table 1, respectively.

For fit1, neither of the considered penalties has an effect even if we were to impose them. They are not imposed as a result: the fit1 curves are identical in the left and right panels.

The form of the penalty is more important for the rest of the fits. For fit 2, in addition to the version with the ReLU prior penalty in the left panel, we alternatively present a version constrained by the AbsLog prior with a weight of $w = 1$. The resulting gluon is displayed in the right panel of Fig. 6, and the χ^2 as well as momentum fractions are listed in the first row of “Alternative fits”, labeled as “fit2alt”, in Table 2. The AbsLog penalty has a smoothly increasing objective function, see Fig. 3, which mildly disfavors even non-zero Bernstein coefficients, $|c_l|$ of $\mathcal{O}(1)$. Consequently, the fit2alt curve in the right panel must be very close to the carrier-only fit1 curve, as its allowed $|c_l|$ are small; the χ^2 of fit2alt in Table 2 is only a tad below that for fit1.

On the other hand, going back to the ReLU penalties in the left panel, the Bernstein coefficients are allowed to grow up to $|c_l| \sim 10$: the fit2 gluon is significantly different from the fit1 gluon, despite the fact that χ^2 values are practically the same for fit1 and fit2. The direct constraint on the gluon is weak. We rather observe the interplay between different flavors, with the rectilinear activation impeding the sea PDF when one of the c_l of the sea saturates the bound of $\mathcal{O}(10)$, hence modifying the χ^2 . As the sea is intertwined with the gluon, both PDFs are affected and result in two different fit1 and fit2, as seen from comparing the fit2 curves in the two panels of Fig. 6.

The ReLU penalties are consequential for fit3 as well. In the left panel, the distinct behaviors of fit3 and fit3Cgfix are mostly due to the ReLU penalty on the suppression power C_g in the large- x power-law falloff $g(x, Q_0) \propto (1-x)^{C_g}$. While C_g can be large in fit3, strongly suppressing $g(x, Q_0)$ across most of the x range, the ReLU penalty disfavors such suppression of fix3Cgfix, and hence it's the prior penalty, not the data, that determines the slower falloff of the fit3Cgfix gluon at $x \rightarrow 1$.

We have also explored the cases for which A_S is determined from the momentum sum rule instead of A_g , that is, for which A_g is a free parameter. Recall that fitting A_g is preferable when the gluon PDF is small, as

Fit name	χ^2	$\langle xg \rangle$	$\langle xS \rangle$	$\langle xV \rangle$	Description
Nominal	446.99	0.228	0.258	0.515	{0,1,1} free CPs, 9 parameters, $\alpha_x = 1$
Change in free CPs	446.99	0.228	0.258	0.515	Free CPs moved from $x = 0.4$ to 0.3
Change in fixed CPs	445.94	0.191	0.307	0.503	Fixed CPs moved, $x = \{10^{-3}, 0.8\} \rightarrow \{0.1, 0.6\}$
$\alpha_x = 0.3$	444.41	0.090	0.482	0.428	α_x changed to 0.3

Table 3: χ^2 values and momentum fractions for a family of fits obtained from the “nominal” baseline by changing the various settings discussed in the text.

is allowed by the contemporary pion data. The last two rows of Table 2 lists settings of two such fits, dubbed “fit1g” and “fit2g” – the counterparts of “fit1” and “fit2alt”. xFitter implements the free- A_g fits with the help of the pdfdecomps/SU3_(PositivePion_) gluon flavor decompositions included in our xFitter branch. We expect that the free- A_S and free- A_g fits to be equivalent when they converge well – and indeed we see such equivalence between the “fit1” and “fit1g”, and “fit2alt” and “fit2g” rows of the Table.

4.3. Channeling flexibility

In this section, we continue to showcase the properties of metamorphs when generating diverse functional forms, now exploring dependence on such inputs as α_x , N_m , or the positions of fixed and free CPs in Eq. (3), still using the pion fits as the example. We take a variation on fit1 and fit2 with even weaker AbsLog penalties with $w = 0.01$. This variation, labeled “Nominal” from now on, has one free CP at $x = 0.4$ for the sea and the valence (no free CP for the gluon), plus two FIXed CPs at $x = 0.001, 0.8$ for every flavor. With our choice of weak penalties, the fit is very similar to the carrier-like result [fit1] shown in the right panel of Fig. 6.

By modifying this nominal result, we will explore three features, namely, the invariance under a relocation of free CPs, variation under a relocation of fixed CPs, and a change due to the stretching power, α_x .

Figure 7 shows the outcomes, for all three flavor combinations, of those three variations available within the Fantômas methodology. The metamorph labeled “Change in free CPs” were obtained modifying the position of the free CP for the sea and the valence from $x = 0.4$ to $x = 0.3$. The corresponding metamorph PDFs (dashed orange curves) did not change compared to the nominal ones (pink solid curves). In these plots, the consecutive curves are shifted upward by 0.025 to distinguish coinciding PDFs.

Hence, given some N_m , positions of free CPs can be moved around without changing the best-fit polynomial solution. The only restriction is that free CPs cannot be too close so as not to introduce numerical instabilities, cf. Appendix B. The invariance of the best-polynomial with respect to the placement of free CPs is mathematically rigorous. Namely, since the best-fit polynomial of a given degree N_m and the given number of free CPs is unique according to the unisolvence theorem, moving the free CPs around does not change this polynomial. Consequently, the PDFs labeled as “Change in free CPs” in Fig. 7 are equivalent to the nominal ones.

The metamorphs labeled “Change in fixed CPs” were obtained by modifying the positions of the fixed CPs of all three combinations from $x = 0.001, 0.8$ in “Nominal” to $x = 0.1, 0.6$. This produces noticeable variations in the metamorph (dotted dark-green curves), as expected.

The metamorphs labeled “ $\alpha_x = 0.3$ ” were obtained by modifying the stretching exponent for all three combinations from $\alpha_x = 1$ in “Nominal” to $\alpha_x = 0.3$. Again, there are noticeable variations in the metamorph (dot-dashed dark-blue curves). The choice of the stretching function $y(x) = x^{\alpha_x}$ thus is a meaningful control to modify the metamorph, together with the choice of N_m and placement of fixed CPs.

How many free parameters? As we increase the flexibility of the parametrization by adding parameters, we eventually reach a low χ^2 value for which the fit effectively stops converging. The unisolvence theorem again explains why this happens – see the discussion in [32]. Namely, as the number of parameters increases, we transit from a single polynomial solution achieving the χ^2 minimum, when the data and prior constraints are constraining enough, to infinitely many solutions with comparably good χ^2 . In some cases, non-convergence may happen, as illustrated with “fit3.” As shown, one may recover the regime with a global minimum of χ^2 by fixing select parameters or adding prior constraints. The representative exploration of a variety of solutions, including higher degree polynomials that

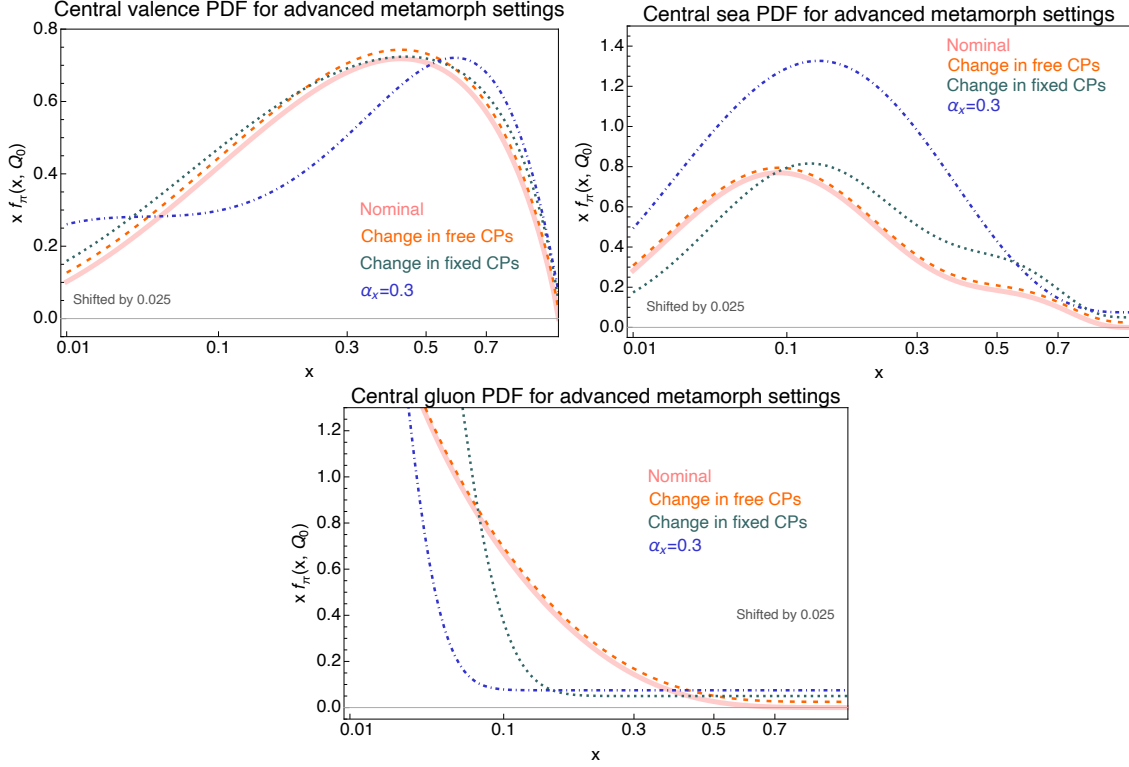


Figure 7: PDFs from fits in Table 3 illustrating the impact of metamorph settings: nominal fit (solid pink), change in all free control points (dotted orange), change in all fixed control points (dashed dark green) and change in α_x (dot-dashed dark blue). See text. The curves are shifted incrementally by 0.025 in the order they appear in the legend.

may introduce redundancy, remains necessary as a part of estimation of the epistemic uncertainty, since the solutions with about the same χ^2 may be equally acceptable. The Fantômas toolkit enables robustness when exploring a range of solutions rather than locking into a potentially over-constrained space. When quantifying the resulting uncertainty, the value of the best χ^2 alone does not constitute a sufficient criterion in favor of a model/fit. In the next Section, we will discuss how various models can be combined to form a PDF ensemble that accounts for the diversity of such parametrizations.

5. Combination of PDF fits

In addition to the central fit corresponding to the global minimum of χ^2 , a global QCD analysis in the Hessian formalism typically provides an ensemble of eigenvector PDF sets to quantify experimental and other sources of the uncertainty. In xFitter, the default criterion to define the 1σ experimental uncertainty for a given PDF parametrization corresponds to a cut in the chi square increase of $\Delta\chi^2 = 1$ above the best-fit value.

However, the final PDF uncertainty must account for the span of acceptable PDF solutions that can be determined using a number of criteria. The most common procedure to combine the PDF solutions with distinct functional forms is based on model averaging using the χ^2 or a related objective function of the type given in Eq. (17). This is the simplest approach, however, associated with the *weak* goodness-of-fit criterion [2] quantifying the *average* agreement of the theoretical model and data. A model satisfying the weak criterion may still fail in some ways, *e.g.*, by disagreeing with subsets of data beyond the level allowed by random fluctuations of data. The *strong* goodness-of-fit criteria [2] are more comprehensive ones; they quantify more detailed comparisons of theory and data, but generally are more difficult to implement. Bayesian model averaging must also generally account for dependence on the priors and can be done, *e.g.*, using the methods adopted in lattice QCD [34] and recently explored for toy PDFs [19]. In such Bayesian

combination, information criteria penalize models with too many parameters. Finally, the combination must account, even reward, for including maximally dissimilar PDF solutions that provide comparable agreement with the fitted data.

For example, in Refs. [25, 26] we selected and combined the representative pion fits, out of about 100 fits with different functional forms, with the help of the mp4lhc package for METAPDF generation [31]. As its name reflects, the package was used for the purpose of the PDF4LHC combination, among other things. Through this procedure, we produced an NLO ensemble Fanto10 of Hessian eigenvector sets that quantifies the sum of experimental (aleatoric), parametrization (epistemic), and (in the most recent version in [26]) nuclear PDF uncertainties. The full Fanto10 PDF combination follows a sequence of procedures A and B outlines below.

5.1. Procedure A. A PDF combination with aleatoric and epistemic uncertainties.

Given the relative paucity of the available pion data, we adapted a simplified procedure for the PDF model combination that accounts for considerations based on the goodness-of-fit criteria described above.

1. For each PDF model \mathbf{M} distinguished by its parametrizations and prior constraints, out of a collection \mathbf{C}_M of such explored models, we find the best fit corresponding to the minimum of $\chi^2 = \chi_{LL}^2 + \chi_{\text{prior}}^2$ given in Eq. (17). We keep the models with the likelihood $\chi_{LL}^2(\mathbf{M})$ satisfying

$$\chi_{LL}^2(\mathbf{M}) \leq \min_{(\mathbf{M} \in \mathbf{C}_M)} \chi_{LL}^2 + \sqrt{2(N_{pts} - N_{par}(\mathbf{M}))}, \quad (19)$$

where $\min_{(\mathbf{M} \in \mathbf{C}_M)} \chi_{LL}^2$ is the lowest log-likelihood $P(D|\mathbf{M})$ for the fitted pion data D among all tried PDF models $\{\mathbf{M}\}$. $\sqrt{2(N_{pts} - N_{par})}$ is one standard deviation on χ_{LL}^2 with $N_{pts} - N_{par}$ degrees of freedom. We note that this selection does consider the prior model penalties in χ_{prior}^2 , viewed as a part of the parametrization.

2. Among the select best fits with low χ^2 , not all result in distinct PDF behaviors. We retain a small number, \tilde{N} , of them that produce distinct PDF shapes, which have been selected by ad-hoc criteria in the current implementation.
3. For each of \tilde{N} retained models, we generate a Hessian uncertainty $\Delta_{LL} f_a(x, Q_0; \mathbf{M})$ according to the textbook criterion $\Delta \chi_{LL}^2 = 1$ at 68% CL. For the pion fit, we choose $\tilde{N} = 5$.
4. We combine the Hessian error bands obtained in the previous step into a single uncertainty using the METAPDF procedure [31] consisting of the following. First, we generate 100 MC replicas from each error band according to the algorithm developed in Ref. [39]. The $100 \cdot \tilde{N}$ replicas are then compressed into a Hessian PDF set using the mp4lhc code, version 2.0. As a part of the pion study, we upgraded this code to support the METAPDF combination for arbitrary hadrons and (anti)quark flavor contents.

As we stated in Ref. [26], probabilistically, the final PDF set at each value of (x, Q^2) corresponds to the sum of the probability of each of the \tilde{N} distributions. Those are independent and have identical statistical properties¹¹. Also, the \tilde{N} models are exchangeable. Hence, the final FantôPDF set can be interpreted as coming from the distribution of a latent variable, *i.e.*, a prior, that captures the underlying influence on the \tilde{N} models – an underlying truth for PDF shapes [40]. This interpretation casts the Fantômas methodology, incremented with the combination à la METAPDF, as effectively capturing the epistemic uncertainty.

5.2. Procedure B. Including uncertainties from other nonperturbative functions

The Fantômas framework can include other types of uncertainties in addition to the ones discussed above. Ref. [26] describes the combination procedure that includes a third-party input with uncertainties, in that particular case, the nCTEQ15 nuclear PDFs [41] required for the computation of cross sections in pion-nuclear Drell-Yan pair production. The nCTEQ15 Hessian PDFs were converted into Monte-Carlo replicas, then the respective variations in the central pion PDFs were absorbed into the final pion+nuclear uncertainty of the respective FantôPDF ensemble

¹¹The Fantômas methodology, along with the combination of sets, ensures that the models are applied independently, and resampling is done independently for each model's output. The METAPDF procedure, as resampling method, ensures that the distributions are identically generated for all models' outputs.

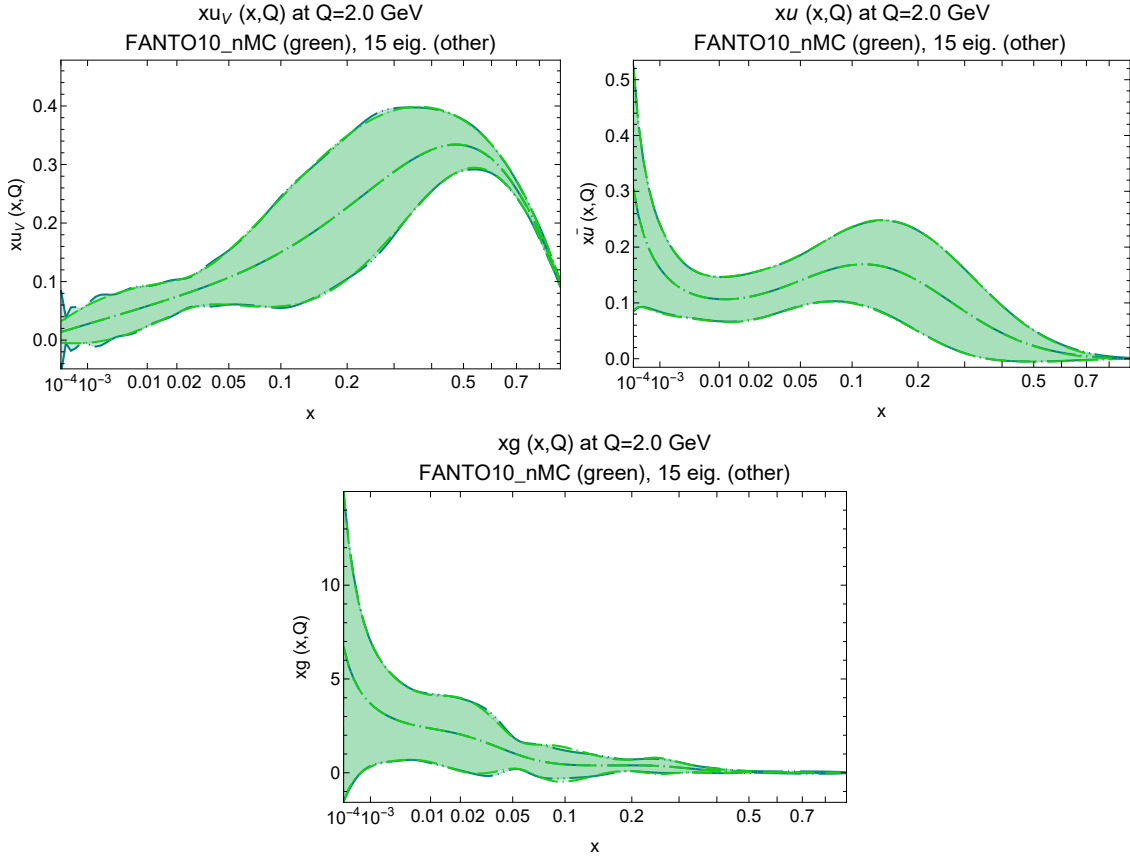


Figure 8: The aleatoric+epistemic+nuclear uncertainties of the published combination of Fanto10_n15 NLO pion PDFs [26] for $xu_v = xV/2$, $x\bar{u} = xS/6$, and xg at QCD scale $Q = 2$ GeV. Light green curves and filled bands represent the average PDFs and uncertainties of the Monte Carlo replica sample at 68% C.L. The darker ones stand for the central PDFs and uncertainty bands obtained by the conversion of the above MC replica set into a Hessian ensemble with 15 eigenvector sets.

using the METAPDF combination. The resulting updated combination for the Fanto10 PDFs [25] are shown in Fig. 8. This figure emphasizes that the final Hessian ensemble approximates well the error bands obtained with intermediate Monte-Carlo replicas, which capture both the variability of the selected central fits due to the Fantômas functional forms, as well as the error bands around each central fit due to the experimental uncertainty. This procedure could be followed for including other uncertainties involving third-party inputs, such as those from fragmentation functions in semi-inclusive DIS.

6. Guidelines

In the previous Sections, we have illustrated the power of the Fantômas methodology. In this Section, we will summarize the “dos and don’ts” to follow.

Dos:

1. Start with low-degree polynomials: Begin by using bare carriers or low-degree polynomials with fixed control points near the endpoints, as outlined in Sec. 4.1.
2. Place fixed control points at the lower and upper ends of the x region probed by the experimental data. Outside of this region, now delineated by the variables x_{min} and x_{max} that were set by placing these CPs, the metamorph will follow the asymptotic behaviors at $x \rightarrow 0$ or $x \rightarrow 1$ that are fully controlled by the carrier.

3. Add control points incrementally: Once a preliminary fit with such basic parametrizations has converged, add one or few NEW CPs according to the sequential approach outlined in Section 4.1 to further improve description of data while maintaining the stable convergence and optimizing fitting time. According to the unisolvence theorem, varying positions of FREE CPs for a fixed N_m does not modify the eventual best-fit metamorph, but it may affect the rate of convergence. Varying numbers and positions of FIXED CPs and the modulator's stretching power α_x (or possibly the whole stretching function $y(x)$) does change the best-fit metamorph. Varying α_x is highly recommended to identify a Bernstein basis that adequately captures the x dependence of data.
4. Set penalties thoughtfully: Implement prior constraints with the `metamorphCollection::Chi2prior()` method and save the files `steering.fantomas.out.txt` and `metamorphCollectionPrior.cc` in the `output/` directory, retaining the metamorph and prior settings for the lowest achieved χ^2 . The resulting solutions may strongly depend on the prior.

Don'ts:

1. Avoid overcomplicated polynomial degrees: Smooth functions of $x \in [0, 1]$ rarely require excessively high polynomial degrees. Although over-fitting is not inevitable, it is possible. Maintain a minimal polynomial degree while ensuring integrability, cf. Sec. 3.6.2, and proper endpoint behavior, as discussed in the “Dos.” For example, in the pion PDF fit, a maximum polynomial degree of $N_m = 3$ was used, beyond which the data struggled to accommodate for additional flexibility/parameters.
2. Beware of oscillatory patterns: One-dimensional Bézier curves are subject to the Runge phenomenon —numerical oscillations arising from equally spaced interpolation points. Mitigate these by:
 - Positioning control points unevenly and at sufficient distance from each other.
 - Adjusting the stretching power α_x to optimize data coverage. Appendix B provides a detailed analysis of numerical artifacts.
3. Monitor condition numbers: Coefficients for Bézier polynomials are computed through inversions of Vandermonde matrices, as shown in equation 11. Numerical stability of solutions is gauged by the condition number. Fantômas evaluates it in `metamorph.cc`, as described in Appendix B, and reports as an error message if the condition number is excessive.

```

1 //check the condition number for T
2 double condnum=MetaVector[NMeta].GetConditionNumber();
3 if (condnum > 10000){
4     cerr << "WARNING: a high condition number ="<<condnum
5         << "in metamorph " << MetaVector[NMeta].ID << endl;
6     cerr << "Check x spacing of its control points" << endl;
7 }

```

Although there is no strict threshold for the condition number, selecting solutions with relatively lower values is advisable to reduce numerical fluctuations and, collaterally, oscillatory effects [42].

7. Conclusions

In global QCD analyses of hadron scattering data, inference of functional forms for nonperturbative functions necessitates comprehensive techniques to systematically span the solution space and quantify associated uncertainties. Neural networks are now commonly used for this purpose, in parallel with the traditional approaches based on analytical parametrizations, but Bézier curves offer a new effective alternative for solving this complex inverse problem. Bézier curves rely on *control points* that determine the shape of the curve and can be algorithmically chosen either by a human or intelligent program. Variation of the control points supplants direct variations of polynomial coefficients and is computationally efficient. We introduced a C++ toolkit Fantômas for generation of PDF parametrizations in the Bézier representation and control of prior constraints on the PDFs. Fantômas can be deployed together with the program `mp4lhc` to create combined uncertainty bands using a variety of Bézier functional forms, or metamorphs, according to the METAPDF PDF combination methodology [31]. This toolkit has been applied to the determination of pion PDFs [25], demonstrating its robustness when implemented inside the xFitter minimization framework.

Section 2 of the article sets up the mathematics of the Bézier polynomial approximants on which the Fantômas methodology is based. Then, Sec. 3 reviewed the components of the Fantômas toolkit and introduced its two realizations as a standalone program or as a module in xFitter. The former was explained in detail with code snippets in Sec. 3.5, and the latter in Sec. 3.6, together with a short description of the C wrapper to simplify interfacing with Fortran in Sec. 3.4.

Section 4 focused on a series of simple fits of pion PDFs demonstrating how to deploy the Fantômas toolkit in practice. We discuss how to progressively increase the flexibility of the functional forms by adding control points and to mitigate non-convergence or overfitting by adding prior penalties using a built-in method of the Fantômas framework, called `Chi2prior()`. Overfitting arises when a model becomes too complex relative to the data. Using flexible functional forms along with adaptive methodologies does not inherently lead to this issue, but requires a systematic tracking, here implemented through priors.

After obtaining converged fits for several sets of metamorph functional forms and respective error bands for experimental uncertainties, we can combine them using the METAPDF technique. Section 5 outlines a procedure for such combination, which includes two main components: Procedure A for the combination of models (*i.e.*, functional forms), guided by information criteria and quantitative indicators such as the likelihood-ratio test, penalties due to the number of parameters, and distances between functions; and Procedure B for inclusion of uncorrelated uncertainties from external sources. The latter is exemplified by the inclusion of nuclear PDF uncertainties in the `Fanto10_n15` NLO error PDFs for the pion presented in a separate publication [26].

To guide the users in efficient generation of the Bézier-based parametrizations, we have compiled a list of “dos and don’ts” in Sec. 6, drawing on the material in the preceding sections and our own experience with fitting such PDFs. This article includes two appendices: Appendix A with an overview of the xFitter network, and Appendix B dedicated to the control of numerical artifacts with polynomials of elevated degree. We conclude that the polynomial approximators are no more prone to numerical instabilities, biases, or overfitting than neural networks are. The Bézier polynomials can approximate smooth 1-dimensional functions to arbitrary accuracy, and they allow for transparent, interpretable exploration of the full diversity of PDF shapes. In practice, low-degree polynomials, enhanced by Bézier curve features such as control points and stretching parameters, are generally sufficient for modeling one-dimensional shapes at $x \in [0, 1]$.

This methodology is developed with an eye on the next generation of precision global analyses of unpolarized PDFs. It may prove useful for modeling other types of non-perturbative functions as well, and it goes along with information-theoretical approaches to quantify the epistemic uncertainty. From a Bayesian perspective, Fantômas facilitates systematic exploration, or sampling, of a wide range of plausible functional forms [32, 43, 44], *i.e.*, marginalizing over the parameter priors [45]. The C++ code deliverables of this project (both the standalone and xFitter implementations) are available from our GitLab repository.

Acknowledgments

We thank the xFitter collaboration members for their assistance with the xFitter program. The authors are extremely thankful to Alim Ablat and Yao Fu for beta testing the standalone code. This study has been financially supported by a National Science Foundation AccelNet project, by the U.S. Department of Energy under Grant No. DE-SC0010129, and by the U.S. Department of Energy, Office of Science, Office of Nuclear Physics, within the framework of the Saturated Glue (SURGE) Topical Theory Collaboration. AC and MPC were partially supported by the UNAM Grant No. DGAPA-PAPIIT IN102225. The work of TJH at Argonne National Laboratory was supported by the U.S. Department of Energy under contract DE-AC02-06CH11357. AC and FO are grateful for the hospitality of the BNL EIC Theory Institute where some of this work was performed. PMN is grateful for support from Wu-Ki Tung Endowed Chair in particle physics. PMN and AC thank the Institute of Nuclear Theory at University of Washington for the hospitality during their work on a part of this project.

Appendix A. Review of the xFitter framework

xFitter is an open-source QCD fitting framework designed to assess the impact of new data on the extracted parton distribution functions (PDFs) and fragmentation functions (FFs). xFitter provides a standard interface to a wide variety

of tools to facilitate comparative studies and evaluate constraints on PDFs/FFs. It has been used for 100+ analyses, including many LHC studies.

xFitter combines experimental data with theoretical calculations to determine the PDFs. The experimental data used in xFitter come from a wide range of sources, including fixed-target and collider experiments. The specific datasets are selected based on the PDFs being studied and the constraints required to define them. After selecting the data, xFitter uses the generated PDFs to compute the theoretical predictions and compare them with the experimental measurements. It optimizes the agreement between the data and theory by modifying the trial PDFs using the MINUIT minimization package from the CERN libraries.

We augmented the xFitter framework by including the Fantômas toolkit for advanced PDF parametrizations, and we extended a fit of NLO PDFs in the pion [28] available in the xFitter examples to explore the parametrization dependence with metamorph parametric forms [25, 26].

The xFitter fitting algorithm is organized into five stages: 1) Initialization, 2) Preparation of data, 3) Theory calculations, 4) QCD analysis, and 5) Output of results. This general structure is illustrated in the flowchart of Fig. A.9. The initialization process declares all necessary variables to be used based on the initial settings. The chosen experimental data sets are compared against the theoretical predictions in the course of the QCD analysis, which calculates and saves the final results at the end.

The main package of xFitter stores a variety of PDF parameterizations, and it is possible to add a custom parameterization as well. We use this option offered by the xFitter’s modular structure to embed the Fantômas parameterization without interference with the other xFitter routines, as Fantômas is (mostly) localized within its own module.

This implementation is a part of the section “3) Theory” of the flowchart of Fig. A.9. Specifically:

- xFitter implements several parameterizations, and these are contained in the `pdfparams/` directory. For example, the `HERAPDF/` directory contains the commonly used HERA PDF parameterization. Fantômas source files are included in `pdfparams/Fantomas/`, as detailed in Sec. 3.6.
- To configure the fit to call the Fantômas parameterization, we modify `parameters.yaml` containing the settings of the fit in the following sections:
 1. **MINUIT**: lists options for the MINUIT fitting routine;
 2. **Parameters**: list and initial values used for the fitted parameters passed to MINUIT. The majority of parameterizations store the initial and final parameters in this section. A Fantômas fit with its distinctive format of parameterizations, on the other hand, requires separate steering cards, `steering_fantomas.txt` and `steering_fantomas_out.txt` to store the initial and current best-fit metamorph parameters and settings, respectively. The **Parameters** section of `parameters.yaml` in this case has a simpler fixed format that stores only the initial nil values for deltas, the changes of the metamorph parameters, as detailed in Secs. 3.6 and 4.1;
 3. **Parametrizations**: call the classes for the chosen parametrization per flavor and lists the parameters to be minimized per flavor. This can be a mix of parameterizations from Fantômas and other parametrization forms, such as HERAPDF;
 4. **Decompositions**: The `parameters.yaml` file also specifies the flavor decomposition for chosen hadron. The available decompositions can be found in `pdfdecomps/`. For the pion fit, either the

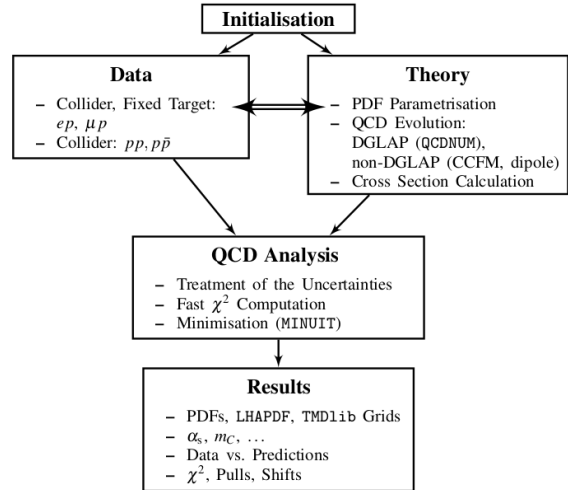


Figure A.9: xFitter schematic organization. (Fig. from Ref. [46])

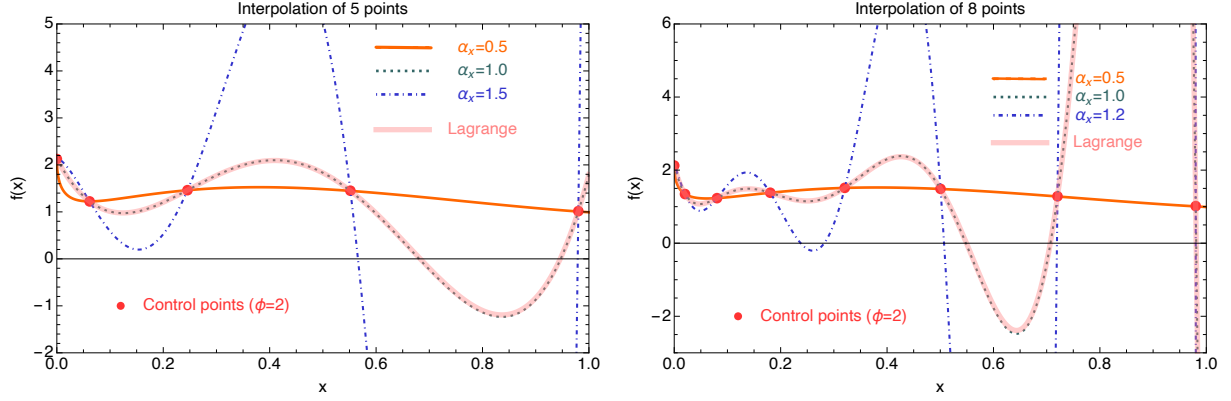


Figure B.10: Effect of the stretching power $\alpha_x = \text{xPower}$ on the shape of the interpolated function and the oscillatory pattern, for 5 points (*l.h.s.*) and 8 points (*r.h.s.*) distributed following Eq. (B.2). The Bézier curves obtained with $\alpha_x = 1$ correspond to the Lagrange interpolation.

SU3_Pion, for π^- , or the SU3_PositivePion, for π^+ , can be chosen if the sea normalization A_S is fitted as a free parameter. If the gluon normalization A_g is fitted instead, the respective decompositions are SU3_Pion_gluon and SU3_PositivePion_gluon;

5. `Evolutions`: specifies the external evolution code, *e.g.*, QCDNUM, or the use of LHAPDF grid, as well as the class for all involved hadrons and their respective PDFs. This part of the file also specifies the choice of QCD parameters and alike, and it calls the file `constants.yaml`; `DefaultEvolution`: sets parameters of the DGLAP evolution;
6. `byReaction`: specifies heavy-quark factorization schemes and relevant QCD parameters by the reaction. For example, at NLO xFitter provides DIS cross sections in the Thorne-Roberts (TR') [47] and ACOT [48, 49] heavy-quark schemes.
7. `WriteLHAPDF6`: sets the header for the LHAPDF grids.

- Within xFitter, the `steering.txt` file specifies which data sets are used.
- The `constants.yaml` file lists all EW parameters as well as quark masses.

To recap, the Fantômas extension retains the general structure of the xFitter framework. Thus, it provides access to the full range of xFitter features, including evaluating functions to compute PDF uncertainties, data pulls, χ^2 values for individual data sets and fitting parameters, as well as to export the results into LHAPDF grids and `xfitter-draw` plotter program. Additional information on the xFitter program can be found in Refs. [30, 46].

Appendix B. Numerical artifacts

Polynomial interpolation is not free of numerical artifacts, one of which is the wiggly or even oscillatory behavior that the interpolating polynomial exhibits under some conditions. When working with flexible polynomials—either by increasing their degree or by the choice and placement of interpolating points—concerns about the smoothness and stability of the interpolation naturally arise.

In the context of Bézier curves, these interpolating points are related to the positions of what, in this manuscript, we call *the control points*. In Section 2.2, we introduced the mathematical formalism of Bézier curves via control points and illustrated their behavior in Section 4. Here, we extend the discussion to analyze how the numerical behavior of the interpolation is affected by the positioning of these control points in our metamorph formalism. To do so, we will analyze two metamorph settings in interpolation mode, which differ by their polynomial degree and the stretching parameter, α_x , illustrated in Fig. B.10. We work with square systems only.

Points	$\alpha_x = 0.5$	$\alpha_x = 1.0$	$\alpha_x = 1.5/1.2$
5	12.2109	42.9459	479.995
8	192.45	2472.02	19683.3

Table B.4: Condition number for the interpolating polynomials of Fig. B.10.

Appendix B.1. Parametric vs. 1D Bézier curves

Bézier curves are full two-dimensional parametric curves $\mathcal{B}(t) = (x(t), y(t))$, $t \in [0, 1]$ — that are defined through a convex hull determined by *external* control points [38]. The control points that define the Bézier hull are connected via de Casteljau’s algorithm to the interpolating points used in our formalism (and which are referred to as *control points* in the manuscript), as detailed in Section 2.2.

The metamorph formalism, however, is not based on the full two-dimensional parametric Bézier curve but rather on its y -projection, denoted as $\mathcal{B}(x)$ with x the coordinate [50], with $N_m + 1$ interpolation points $\{x_i, \mathcal{B}^{(N_m)}(y(x_i))\}$, $i = 1, \dots, N_m + 1$, effectively reducing to a one-dimensional interpolation, and is thus subject to numerical artifacts similar to those observed in other polynomial interpolation schemes.

In what follows, we will continue to refer to these interpolation points as control points (CPs), consistent with the terminology used throughout the manuscript. Note that, in contrast to classical parametric Bézier curves, the resulting metamorph function passes exactly through its CPs.

Appendix B.2. Condition Number and Matrix Inversion in Polynomial Interpolation

Multiple criteria were tested to determine the optimal values of Fantômas’ parameters in order to produce acceptable solutions, particularly to avoid undesired wiggleness. Oscillatory patterns are closely tied to the behavior of the transformation matrix, which in our case is the product of the T and the M matrices. The T -matrix naturally arises in polynomial interpolations; its entries are successive powers of the control points. Matrices with this structure are called *Vandermonde matrices*, whose stability and conditioning have been extensively studied [42, 51, 52]. The product $\underline{T} \cdot \underline{M}$ forms the coefficient matrix of the linear system that must be solved to fully determine the interpolating polynomial. The stability of the interpolation is determined by this composed matrix. The stability of these fits can be assessed by the condition number

$$\kappa(\underline{A}) = \|\underline{A}\| \|\underline{A}^{-1}\|, \quad (\text{B.1})$$

with $\|\underline{A}\| = \sum_{i=1}^n \|\underline{A}_i\|_2 = \sum_{i=1}^n \left(\sum_{j=1}^m |A_{j,i}|^2 \right)^{1/2}$. This quantity measures the amplification of input perturbations in the output, reflecting whether the matrix $\underline{T} \cdot \underline{M}$ is *ill* or *well*-conditioned. Matrices with large condition numbers are prone to substantial output variations from small input perturbations, leading to numerical instability. Consequently, large condition numbers are undesirable, yet they do not always correlate with oscillatory patterns. Optimizing the condition number becomes a delicate balance between choosing the number of control points and their positions, which is a hallmark of the Runge phenomenon that will be discussed hereafter. Table B.4 provides the condition numbers for the six interpolating functions illustrated in Fig. B.10. We observe that the condition number is larger for curves with more pronounced oscillations. However, this comparison is relative for each setting, *e.g.*, for each value of N_m . Because \underline{M} has a fixed form once N_m is set, optimizing the condition number relies solely on how \underline{T} is configured [53].

Moreover, the inversion of the matrix \underline{T} is computationally costly for high values of N_m . We adopted the LU-decomposition method, implemented in a separate header file, LUPinverse.h. This file contains a function for inverse calculation, which is called in the main code wherever matrix inversion is needed. The inversion time for various $N_m + 1$ points are given in Table B.5.

Appendix B.3. Runge Phenomenon in Polynomial Interpolation

A classical example of interpolation instability is the Runge phenomenon, characterized by large variations in the derivatives of an interpolating function near its end-points when evaluated at equidistantly spaced or evenly

Points	LU Decomposition
10	0.0007s
15	0.085s
20	2.221s
25	1m11.723s
30	38m

Table B.5: Time required for \underline{T} matrix inversion with the LU decomposition method.

distributed nodes. For squared systems like the ones considered in Section 2.2, two equivalent closed-form solutions to the interpolation problem exist— one is based on Lagrange polynomials and the other on generalized Bernstein polynomials (see Ref. [32] for details).

The Runge phenomenon is generally illustrated using the Lagrange polynomial-based interpolation. The full 2D parametric Bézier curves are known to avoid such spurious effects, while it is not the case for the 1D metamorph. The latter share characteristics with Lagrange polynomial interpolation. Nonetheless, the flexibility in the choice of control points and scaling of the argument of the Bernstein polynomial, through α_x in Eq. (4), allows some mitigation of these Runge artifacts. In Fig. B.10, we illustrate the behavior of interpolating curves through our formalism for 5 and 8 evenly distributed control points, following

$$x_i = \left(x_{\min} + \frac{x_{\max} - x_{\min}}{N_m} i \right)^\phi, \text{ for } i = 0, \dots, N_m. \quad (\text{B.2})$$

with $\phi = 2$, are chosen from a known reference or “truth” function, and then these are interpolated for various values of α_x . The case $\alpha_x = 1$ corresponds to the standard Lagrange polynomial interpolation and exhibits oscillations for N_m as low as 4 (left panel). By tweaking α_x , we reduce the wiggly pattern, a reduction also reflected in improved condition numbers. The optimal choice to minimize the appearance of high derivatives is ($\phi = 2, \alpha_x = 0.5$).

For practical use of the Fantômas framework, caution is advised when increasing the degree of the polynomial substantially, especially when evenly spaced control points are chosen. For this study, we have explored the possibility of oscillatory solutions, and found them difficult to induce. Notably, no such patterns were observed in the first physics application of the Fantômas framework, *i.e.*, the analysis of the pion PDFs [25] where the highest degree setting was $N_m = 3$ with unevenly spaced control points. It is important to note that oscillations, when they occur, are not necessarily spurious numerical artifacts.

Appendix C. A Mathematica implementation

Our methodology is best illustrated through simple interpolation examples, *e.g.*, as proposed in Ref. [32] to study the large- x behavior of proton PDFs. For that purpose, Fig. C.11 provides a Wolfram Mathematica implementation of the Bézier polynomials that are a part of metamorph modulators. The `Bezier` module can easily be extended to include minimization instead of interpolation. Here, it is shown for $x f(x) = F_a^{\text{car}}(x) \times \mathcal{B}^{(N_m)}(x^{\alpha_x})$, and can easily be adapted to other implementations.

References

- [1] S. Amoroso, et al., Snowmass 2021 Whitepaper: Proton Structure at the Precision Frontier, Acta Phys. Polon. B 53 (12) (2022) 12–A1. [arXiv:2203.13923](#), [doi:10.5506/APhysPolB.53.12-A1](#).
- [2] K. Kovařík, P. M. Nadolsky, D. E. Soper, Hadronic structure in high-energy collisions, Rev. Mod. Phys. 92 (4) (2020) 045003. [arXiv:1905.06957](#), [doi:10.1103/RevModPhys.92.045003](#).
- [3] J. J. Ethier, E. R. Nocera, Parton Distributions in Nucleons and Nuclei, Ann. Rev. Nucl. Part. Sci. 70 (2020) 43–76. [arXiv:2001.07722](#), [doi:10.1146/annurev-nucl-011720-042725](#).
- [4] J. G. Morfin, W.-K. Tung, Parton distributions from a global QCD analysis of deep inelastic scattering and lepton pair production, Z. Phys. C 52 (1991) 13–30. [doi:10.1007/BF01412323](#).

```

1  Fc[x_, {a0_, a1_, a2_}] := a0*x^a1 (1 - x)^a2;
2
3  Bezier[xPower_ : 1, k_ : 1, n_ : 1, q0_ : 1.3] :=
4  Module[{m, nlist, M, t, T, p, l, x, P, C, f, b, B, pts, plotmod,
5    errrplotmod},
6    Params = List[];
7    AppendTo[Params, xPower];
8    AppendTo[Params, k];
9    AppendTo[Params, n];
10   AppendTo[Params, q0];
11   nlist = Range[0, n];
12   m[p_, l_] := (-1)^(p - l) Binomial[n, l] Binomial[n - l, n - p];
13   M = Array[m, {n + 1, n + 1}, {{0, n}, {0, n}}];
14   t[x_, p_] := x^(p*xPower);
15   T = ArrayReshape[
16     Table[t[x, p], {x, xlist}, {p, nlist}], {k + 1, n + 1}];
17   P = ArrayReshape[pdflist/Fc[xlist, auV], {k + 1, 1}];
18   C = Inverse[M] . Inverse[Rationalize[Transpose[T] . T, 0]] .
19     Transpose[T] . P;
20   coef = C;
21 ]
22
23 FBezier[x_, xPower_, n_, coef_] :=
24 Sum[coef[[nu + 1, 1]]*
25   Binomial[n, nu] x^(nu*xPower) (1 - x^xPower)^(n - nu), {nu, 0, n}];

```

Figure C.11: A Mathematica implementation of the Bézier polynomial.

- [5] T.-J. Hou, et al., New CTEQ global analysis of quantum chromodynamics with high-precision data from the LHC, *Phys. Rev. D* 103 (1) (2021) 014013. [arXiv:1912.10053](#), [doi:10.1103/PhysRevD.103.014013](#).
- [6] S. Bailey, T. Cridge, L. A. Harland-Lang, A. D. Martin, R. S. Thorne, Parton distributions from LHC, HERA, Tevatron and fixed target data: MSHT20 PDFs, *Eur. Phys. J. C* 81 (4) (2021) 341. [arXiv:2012.04684](#), [doi:10.1140/epjc/s10052-021-09057-0](#).
- [7] R. D. Ball, et al., Parton distributions from high-precision collider data, *Eur. Phys. J. C* 77 (10) (2017) 663. [arXiv:1706.00428](#), [doi:10.1140/epjc/s10052-017-5199-5](#).
- [8] R. D. Ball, et al., The PDF4LHC21 combination of global PDF fits for the LHC Run III, *J. Phys. G* 49 (8) (2022) 080501. [arXiv:2203.05506](#), [doi:10.1088/1361-6471/ac7216](#).
- [9] R. D. Ball, et al., The path to proton structure at 1% accuracy, *Eur. Phys. J. C* 82 (5) (2022) 428. [arXiv:2109.02653](#), [doi:10.1140/epjc/s10052-022-10328-7](#).
- [10] J. McGowan, T. Cridge, L. A. Harland-Lang, R. S. Thorne, Approximate N³LO parton distribution functions with theoretical uncertainties: MSHT20a N³LO PDFs, *Eur. Phys. J. C* 83 (3) (2023) 185, [Erratum: *Eur.Phys.J.C* 83, 302 (2023)]. [arXiv:2207.04739](#), [doi:10.1140/epjc/s10052-023-11236-0](#).
- [11] R. D. Ball, et al., The path to N³LO parton distributions, *Eur. Phys. J. C* 84 (7) (2024) 659. [arXiv:2402.18635](#), [doi:10.1140/epjc/s10052-024-12891-7](#).
- [12] A. Ablat, et al., New results in the CTEQ-TEA global analysis of parton distributions in the nucleon, *Eur. Phys. J. Plus* 139 (12) (2024) 1063. [arXiv:2408.04020](#), [doi:10.1140/epjp/s13360-024-05865-x](#).
- [13] T. Cridge, et al., Combination of aN³LO PDFs and implications for Higgs production cross-sections at the LHC, *J. Phys. G* 52 (2025) 6. [arXiv:2411.05373](#), [doi:10.1088/1361-6471/adde78](#).
- [14] A. Courtoy, J. Huston, P. Nadolsky, K. Xie, M. Yan, C. P. Yuan, Parton distributions need representative sampling, *Phys. Rev. D* 107 (3) (2023) 034008. [arXiv:2205.10444](#), [doi:10.1103/PhysRevD.107.034008](#).
- [15] B. Kriesten, T. J. Hobbs, Learning PDFs through interpretable latent representations in Mellin space, *Phys. Rev. D* 111 (1) (2025) 014028. [arXiv:2312.02278](#), [doi:10.1103/PhysRevD.111.014028](#).
- [16] B. Kriesten, J. Gomprecht, T. J. Hobbs, Explainable AI classification for parton density theory, *JHEP* 11 (2024) 007. [arXiv:2407.03411](#), [doi:10.1007/JHEP11\(2024\)007](#).
- [17] B. Kriesten, T. J. Hobbs, Anomalous electroweak physics unraveled via evidential deep learning (12 2024). [arXiv:2412.16286](#).
- [18] B. Kriesten, A. NieMiera, W. Good, T. J. Hobbs, H.-W. Lin, Decoding the proton's gluonic density with lattice QCD-informed machine learning (7 2025). [arXiv:2507.17810](#).
- [19] M. Yan, T.-J. Hou, Z. Li, K. Mohan, C. P. Yuan, A generalized statistical model for fits to parton distributions (6 2024). [arXiv:2406.01664](#).
- [20] M. N. Costantini, M. Madigan, L. Mantani, J. M. Moore, A critical study of the Monte Carlo replica method, *JHEP* 12 (2024) 064. [arXiv:2404.10056](#), [doi:10.1007/JHEP12\(2024\)064](#).
- [21] M. N. Costantini, L. Mantani, J. Moore, M. Ubiali, Bayesian combination and determination of pdfs, *pDF4LHC 2024 meeting* (2024). URL <https://indico.cern.ch/event/1435677/>

- [22] G. Cybenko, Approximation by superpositions of a sigmoidal function, *Mathematics of Control, Signals and Systems* 2 (4) (1989) 303. doi:10.1007/BF02551274. URL <https://doi.org/10.1007/BF02551274>
- [23] K. Hornik, M. Stinchcombe, H. White, Universal approximation of an unknown mapping and its derivatives using multilayer feedforward networks, *Neural Networks* 3 (5) (1990) 551. doi:[https://doi.org/10.1016/0893-6080\(90\)90005-6](https://doi.org/10.1016/0893-6080(90)90005-6). URL <http://www.sciencedirect.com/science/article/pii/0893608090900056>
- [24] K. Hornik, Approximation capabilities of multilayer feedforward networks, *Neural Networks* 4 (2) (1991) 251. doi:[https://doi.org/10.1016/0893-6080\(91\)90009-T](https://doi.org/10.1016/0893-6080(91)90009-T). URL <http://www.sciencedirect.com/science/article/pii/089360809190009T>
- [25] L. Kotz, A. Courtoy, P. Nadolsky, F. Olness, M. Ponce-Chavez, Analysis of parton distributions in a pion with Bézier parametrizations, *Phys. Rev. D* 109 (7) (2024) 074027. arXiv:2311.08447, doi:10.1103/PhysRevD.109.074027.
- [26] L. Kotz, A. Courtoy, P. Nadolsky, M. Ponce-Chavez, Fantômas: epistemic and nuclear uncertainties for the parton distributions of the pion (5 2025). arXiv:2505.13594.
- [27] P. C. Barry, N. Sato, W. Melnitchouk, C.-R. Ji, First Monte Carlo Global QCD Analysis of Pion Parton Distributions, *Phys. Rev. Lett.* 121 (15) (2018) 152001. arXiv:1804.01965, doi:10.1103/PhysRevLett.121.152001.
- [28] I. Novikov, et al., Parton Distribution Functions of the Charged Pion Within The xFitter Framework, *Phys. Rev. D* 102 (1) (2020) 014040. arXiv:2002.02902, doi:10.1103/PhysRevD.102.014040.
- [29] P. C. Barry, C.-R. Ji, N. Sato, W. Melnitchouk, Global QCD Analysis of Pion Parton Distributions with Threshold Resummation, *Phys. Rev. Lett.* 127 (23) (2021) 232001. arXiv:2108.05822, doi:10.1103/PhysRevLett.127.232001.
- [30] xFitter, The xFitter project is an open source QCD fit framework ready to extract PDFs and assess the impact of new data., <https://www.xfitter.org/xFitter/>.
- [31] J. Gao, P. Nadolsky, A meta-analysis of parton distribution functions, *JHEP* 07 (2014) 035. arXiv:1401.0013, doi:10.1007/JHEP07(2014)035.
- [32] A. Courtoy, P. M. Nadolsky, Testing momentum dependence of the nonperturbative hadron structure in a global QCD analysis, *Phys. Rev. D* 103 (5) (2021) 054029. arXiv:2011.10078, doi:10.1103/PhysRevD.103.054029.
- [33] L. A. Harland-Lang, T. Cridge, R. S. Thorne, A Stress Test of Global PDF Fits: Closure Testing the MSHT PDFs and a First Direct Comparison to the Neural Net Approach (7 2024). arXiv:2407.07944.
- [34] W. I. Jay, E. T. Neil, Bayesian model averaging for analysis of lattice field theory results, *Phys. Rev. D* 103 (2021) 114502. arXiv:2008.01069, doi:10.1103/PhysRevD.103.114502.
- [35] P. D. Dauncey, M. Kenzie, N. Wardle, G. J. Davies, Handling uncertainties in background shapes: the discrete profiling method, *JINST* 10 (04) (2015) P04015. arXiv:1408.6865, doi:10.1088/1748-0221/10/04/P04015.
- [36] A. Malinin, M. Gales, Predictive uncertainty estimation via prior networks (2018). arXiv:1802.10501. URL <https://arxiv.org/abs/1802.10501>
- [37] G. Farin, *Curves and surfaces for CAGD: A practical guide*, Morgan Kaufmann, 2001.
- [38] M. P. Kamermans, A primer on Bézier curves, <https://pomax.github.io/bezierinfo> (2011).
- [39] T.-J. Hou, et al., Reconstruction of Monte Carlo replicas from Hessian parton distributions, *JHEP* 03 (2017) 099. arXiv:1607.06066, doi:10.1007/JHEP03(2017)099.
- [40] B. De Finetti, Foresight: Its logical laws, and its subjective sources, *Studies in Subjective Probability* 1 (1) (1937) 1–68.
- [41] K. Kovarik, et al., nCTEQ15 - Global analysis of nuclear parton distributions with uncertainties in the CTET framework, *Phys. Rev. D* 93 (8) (2016) 085037. arXiv:1509.00792, doi:10.1103/PhysRevD.93.085037.
- [42] W. Gautschi, On inverses of vandermonde and confluent vandermonde matrices iii, *Numerische Mathematik* 29 (4) (1978) 445–450. doi:10.1007/BF01432880. URL <https://doi.org/10.1007/BF01432880>
- [43] X.-L. Meng, Statistical paradises and paradoxes in big data (I): Law of large populations, big data paradox, and the 2016 US presidential election, *The Annals of Applied Statistics* 12 (2) (2018) 685. doi:10.1214/18-AOAS1161SF.
- [44] A. Courtoy, P. Nadolsky, From Data Defects to Response Functions: A View From Particle Physics, *Harvard Data Science Review* 5 (3), <https://hdsr.mitpress.mit.edu/pub/qp47w8cm> (sep 28 2023).
- [45] L. Del Debbio, Bayesian approach for inverse problems, pDF4LHC 2024 meeting (2024). URL <https://indico.cern.ch/event/1435677/>
- [46] S. Alekhin, et al., HERAFitter, *Eur. Phys. J. C* 75 (7) (2015) 304. arXiv:1410.4412, doi:10.1140/epjc/s10052-015-3480-z.
- [47] R. S. Thorne, A Variable-flavor number scheme for NNLO, *Phys. Rev. D* 73 (2006) 054019. arXiv:hep-ph/0601245, doi:10.1103/PhysRevD.73.054019.
- [48] M. A. G. Aivazis, J. C. Collins, F. I. Olness, W.-K. Tung, Leptoproduction of heavy quarks. 2. A Unified QCD formulation of charged and neutral current processes from fixed target to collider energies, *Phys. Rev. D* 50 (1994) 3102–3118. arXiv:hep-ph/9312319, doi:10.1103/PhysRevD.50.3102.
- [49] T. Stavreva, F. I. Olness, I. Schienbein, T. Jezo, A. Kusina, K. Kovarik, J. Y. Yu, Heavy Quark Production in the ACOT Scheme at NNLO and N3LO, *Phys. Rev. D* 85 (2012) 114014. arXiv:1203.0282, doi:10.1103/PhysRevD.85.114014.
- [50] E. A. López Rosa, Global analysis of a twist-3 parton distribution function with theoretical constraints, Master’s Thesis (2025). URL <https://tesiunam.dgb.unam.mx/>
- [51] W. Gautschi, On inverses of vandermonde and confluent vandermonde matrices, *Numerische Mathematik* 4 (1) (1962) 117–123. URL <https://doi.org/10.1007/BF01386302>
- [52] W. Gautschi, Norm estimates for inverses of vandermonde matrices, *Numerische Mathematik* 23 (4) (1974) 337–347. doi:10.1007/BF01438260. URL <https://doi.org/10.1007/BF01438260>
- [53] Fantômas Team, work in progress (2025).